An Investigation on The Impacts of Inverter Modulation Techniques on The Performance of The Dual Inverter Drive

by

Mohammed Sleiman

Bachelor of Electrical Engineering, Beirut Arab University, 2018

Submitted to the Graduate Faculty of the

Swanson School of Engineering in partial fulfillment

of the requirements for the degree of

Master of Science in Electrical and Computer Engineering

University of Pittsburgh

2020

UNIVERSITY OF PITTSBURGH

SWANSON SCHOOL OF ENGINEERING

This thesis was presented

by

Mohammed Sleiman

It was defended on

March 23, 2020

and approved by

Brandon Grainger, PhD, Assistant Professor, Department of Electrical and Computer Engineering

Robert Kerestes, PhD, Assistant Professor, Department of Electrical and Computer Engineering

Zhi-Hong Mao, PhD, Professor, Department of Electrical and Computer Engineering

Thesis Advisor: Brandon Grainger, PhD, Assistant Professor, Department of Electrical and Computer Engineering

An Investigation on The Impacts of Inverter Modulation Techniques on The Performance of The Dual Inverter Drive

Mohammed Sleiman, MS

University of Pittsburgh, 2020

This work presents a comprehensive overview about the dual inverter drives in applications related to the electric vehicle industry. The requirement of efficient and integrated power electronic converter circuits has become an essential requirement to the vehicle function. Major research and progress have been made to achieve dual and bidirectional operation of power flow, while minimizing losses, volume and costs. This thesis surveys the single, three phase, and dual inverter structure and operation. The dual structures are earning growing attention due to their capability to provide multiple output voltages to the stator of the electric machine associated with the electric vehicle. The contribution of this work is to study the impact of the major modulation techniques on the regulated, dual inverter drive performance. The selected methods for evaluation include sinusoidal pulse width modulation, third harmonic injection pulse width modulation, and space vector modulation in terms of the drive's output voltage, fundamental voltage and total harmonic distortion. The second investigation involves the manipulation of phase angle relationships between the gates of the two adjacent inverters, allowing the drive to achieve equal phase voltage and power between both inverters at varying loads.

Table of Contents

List of Tables

List of Figures

Acknowledgements

My deep gratitude goes to my incredible parents, Daad and Omar, who gave me a meaningful life. Thank you for the unconditional love.

My appreciation extends to my hosts, Diana and Raymond, for their unwavering support. I was very fortunate to know amazing people like you.

I'm grateful to the U.S. Department of State for awarding me the Fulbright Fellowship to pursue my graduate degree. Thank you AMIDEAST team for facilitating my study.

I'm indebted for this beautiful country experience, including arts, adventures and opportunities. The American values of inclusion and generosity are overwhelming.

Finally, I'd like to thank my caring Pitt faculty, thesis committee and friends who accompanied me throughout this journey. It's a lifetime pride to be a member in this thriving University community.

Whether near, far, or in heaven, my thoughts are with everyone who made this dream come true.

1.0 Introduction

1.1 History of Dual Inverters

The electrical vehicles industry is booming in 2019, despite all the technical and commercial warnings. This movement is being fostered by electric vehicles low environmental impact, improved driving efficiency and decreasing operational costs. That led EVs (Electric Vehicles) to be an impending alternative to the traditional combustion engine cars [1]. However, the charging architecture and operational range limitation still invoke menacing threat to the EV market expansion. Tremendous efforts have been addressed to reduce the charging cost while considering the energy storage elements' efficiency, size, volume and the bidirectional power transfer from grid to vehicle (G2V), vehicle to grid (V2G) and vehicle to vehicle (V2V)[2].

Then, the integrated onboard chargers seemed to be suitable to resolve various problems. Due to their minimal added circuitry, such topologies are characterized by fast charging capabilities, bidirectional power transfer and low switching stress. Single and dual inverters' schemes were analyzed too [3].

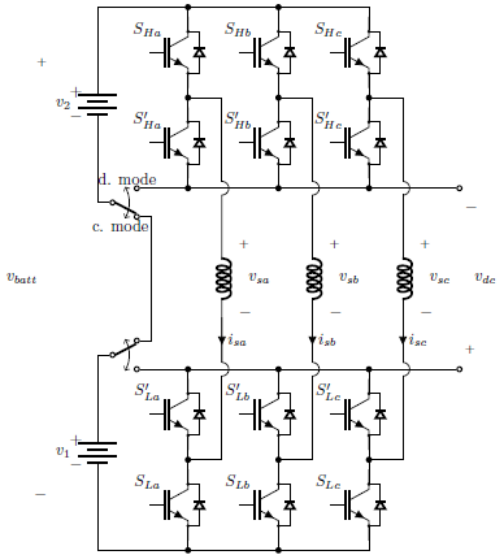

Figure 1 Dual Inverter [3]

Some researchers believe that charging and traction do not occur concurrently [4]. Thus, this necessitates that the charging and traction modes share the same converter to perform any bidirectional operation. However, we may not disregard the issue of common mode noise current that pops up during charging or V2G mode, because the grid is always grounded [5]. To solve that problem, a transformer was used for isolation in many topologies. The usage of transformers led to notable increase in the size and cost of the chargers. To mitigate that, some transformer-less schemes might involve additional switches to bypass the freewheeling currents. Four-wheel-drives entailing EV circuitry were employed to reduce the currents [6].

The integration of the drivetrain into the charging system was first introduced by D. Thimmesch in 1985 [7]. Since then, numerous topologies were proposed to soothe the problematic of integrated chargers. The major concerns were the different voltage levels, torque production, fault protection and charger size.

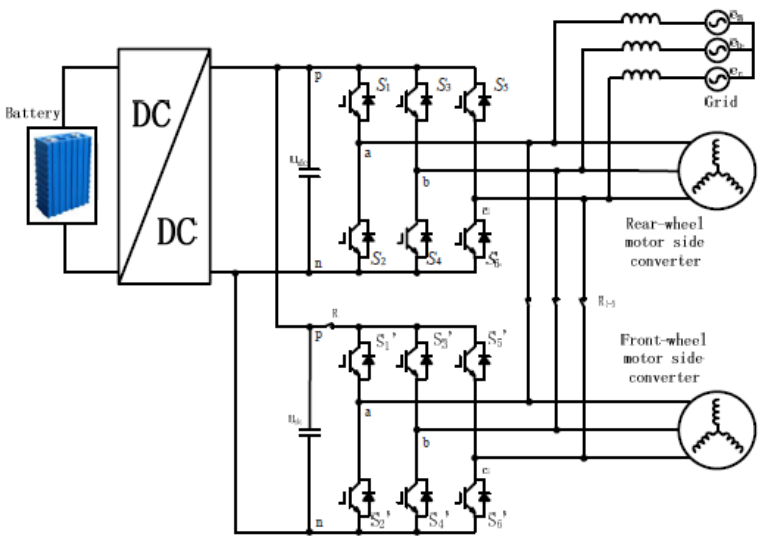

Figure 2 Integrated Three Phase Charger Topology [6]

For instance, the charger introduced in [8] utilizes the machine leakage inductance as a filter to boost converter. The battery voltage must be higher than the maximum line to line voltage of grid and a filter is required to eliminate line current switching ripple. Another charger was proposed based on split phase motor where the stator is configured as a double three phase windings through a relay-based switching device. This scheme was not compatible with market needs, since all charges based on split phase machines require redesign of motors, thus increasing manufacturing costs [8]. Other isolated integrated charger was proposed in [9], while it leads to galvanic isolation between grid and battery, it requires considerable magnetization current due to the presence of an air gap.

Probably the most recent advance in integrated chargers was created by [10], who formulated a fast dc charger including an open winding motor and dual inverter drive. The system implements charge balance by setting different duty cycles to the top and bottom switches. This design drawback is that it does not offer fault blocking capability in case the energy storage sources

voltage was lower than the input voltage. Other study [3] proposed a modified design which can be executed in single or dual inverter architecture. It presents the usage of Single Pole Double Throw (SPDT) contractors to enable the reconfigurations between driving and charging modes. Also, it permits buck-boost operations of high voltages with fault blocking possibility by the impact of body diodes of complimentary switches. Then, the system will be valid for V2G and G2V modes.

Another study [6] examined thoroughly the common mode leakage current paths during charging and V2G operation. The lack of an isolation transformer caused leakage current consisting of the parasitic capacitance between ground, battery and the EV circuit. Upon analyzing a 6-switch inverter operation in high frequency, the common mode voltage fluctuations invoked leakage currents in the circuit depending on the switching state. To eliminate those currents, the common mode voltage fluctuations must be reduced significantly. That might be implemented by different modulation techniques of an NPC inverter for instance. However, such an inverter has 12 switches and 6 diodes, which demand increasing the size and cost of the overall charger.

The latest model was proposed by introducing a typical structure of four-wheel drive EV. It includes the usage of 2 tractions converters connected to the battery in parallel. The power flow is sustained for bidirectional operation through one converter to deliver power from battery to grid in traction or V2G mode and from grid to battery in charging mode. The other converter works only in traction mode to drive the front wheels of the system. In that system, the outputs of the converters' phase legs are connected by 3 relays which will be open or closed reliant on the operation scheme. For example, in the traction mode, the relays will be disconnected, and the motors will operate individually. While in charging or V2G operation, the relays are closed and the battery transfers energy with the grid. A relay will be disconnected to annul the influence of

DC voltage on front wheel. Moreover, in the freewheeling period, when some switches will be off and others connected to grid, a path for currents will be present. Thus, common mode voltages will decrease significantly upon employing certain space vector modulation technique. In addition to that, the system might be functional for single or three phase charging topologies. In conclusion, the efficiency will increase because the conduction losses are lower now and the system volume and weight are abridged [6].

1.2 Motives of Research

As described above, the dual inverters have developed through different stages. The main concern was to obtain the highest possible output voltage with the least possible harmonics. In this study, two elements are being investigated:

1- The prominent modulation techniques and dual inverter operation: three major modulation techniques will be tested on the three-phase inverter. The focus will be on the sinusoidal pulse width modulation, third harmonic injected sinusoidal pulse width modulation and space vector modulation. Upon analyzing the outcomes, the best modulation techniques will be used for several testing trials on the dual inverter drive.

2- The impact of phase angle on dual inverter operation: since two independent inverters will be running to drive the system, there should be certain control to alter the operation of both inverters to obtain the desired voltage, current , power or even harmonics on one or both loads. The gates angle will vary by increments of 30 degrees from 0 to 180 degrees. Also, voltage control and current filtration will be considered.

1.3 Scope of Study

The study begins with performing a literature review of the single-phase inverters, including half and full bridge types. Then, it moves on to survey the three phase inverters. After that, a comprehensive review of the major modulation techniques will be made. Then, the proposed model will be presented. Later on, the simulation section begins by testing the three-phase inverter by the different modulation techniques. The modulation techniques will be tested also on the dual inverter drive, analyzing different cases of operation, phase angle effect, resistance impact, ground current filtration, and methods of voltage control.

2.0 Background

2.1 Inverters

An inverter is a power electronics equipment that converts direct current (DC) power to alternating current (AC) power. Since an inverter can control the voltage and frequency of AC power at any value, it is essential for AC motor drives that require variable voltage and variable frequency.

Inverters can be classified into two groups based on the type of DC input source: Voltage source inverter (VSI) and current source inverter (CSI).

VSIs are powered by DC voltage sources. At the DC link side of the VSI, there is a shunt capacitor to smooth the DC input voltage. Since the VSI uses a voltage source, if its output terminals are short-circuited, then the possibility of flow of massive current will be high. In contrast, the CSIs are powered by DC current sources, and the danger becomes high when the circuit is opened because a high voltage can be produced.

The inverters are used in two major applications: AC motor drives and AC power supplies. The inverter of AC motor drives varies both the amplitude and frequency of AC voltages. This is often called Variable Voltage Variable Frequency Drive. The AC power supplies inverter demands a fixed amplitude and frequency of the output voltages, since its application acts as a replacement for the mains power. This type is called Constant Voltage Constant Frequency Drive.

2.1.1 Single Phase Inverters

2.1.1.1 Single Phase Half Bridge Inverter

This is the simplest inverter that generates single phase AC voltage from a DC source. The inverter consists of one basic circuit. We can simply produce AC voltage from this inverter by turning the two switches alternatively on and off every half period (T/2). An inverter that uses this modulation is called square wave inverter. In this case, the inverter produces the maximum output voltage. The phase voltage V_p is equal to the load output voltage V_o.

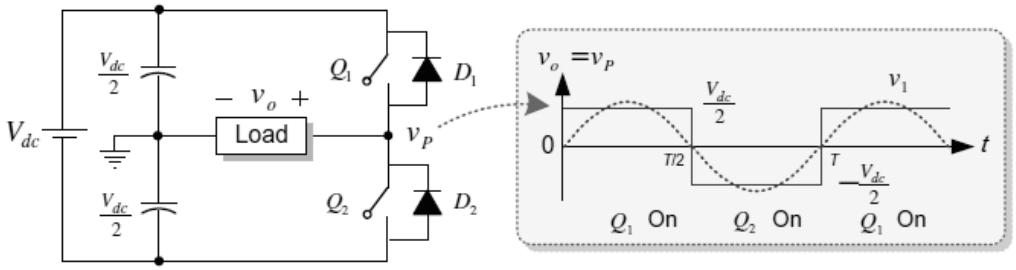

Figure 3 Single Phase Half Bridge Inverter [11]

The phase voltage is not a pure sinusoidal but a square wave which contains many harmonics in addition to the fundamental. By Fourier series, the phase voltage can be expressed as:

$$V_p = \frac{2Vdc}{\pi} \sum_{n=1,3,5\ldots}^{\infty} \frac{\sin nwt}{n} \qquad (2 - 1)$$

Out of all frequency components, only the fundamental can supply effective power to the load. The harmonics will be converted into unnecessary losses or noise. The most dangerous harmonics are the third, fifth and seventh harmonics because of the distortion they cause. Thus, a

low pass filter is used to filter them. To measure the amount of distortion, the Total Harmonic Distortion (THD) is calculated, where f_1 donates the fundamental and f_h is the rest of harmonics, all in rms values.

$$THD = \sqrt{\frac{\sum_{h>1}^{\infty} f_{h,rms}^2}{f_{1,rms}^2}} \times 100\% \qquad (2 - 2)$$

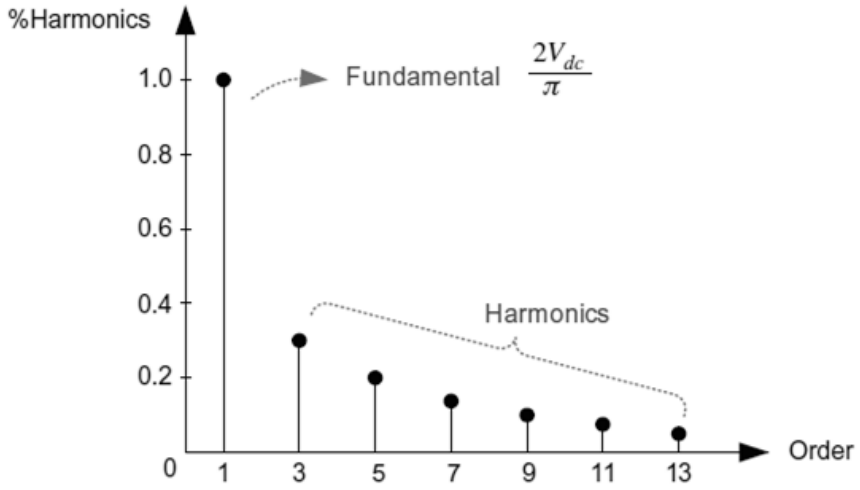

Figure 4 Harmonics in Phase Voltage [11]

2.1.1.2 Single Phase Full Bridge Inverter

The main defect of the half bridge inverter is its low voltage utilization rate which is $0.45V_{dc.}$ The full bridge inverter can duplicate that output voltage to $0.9V_{dc}$. It consists of two basic circuits with four switches. To produce output voltage, there should be 180 degrees difference between the phase voltages. The inverter and switching patterns are shown below:

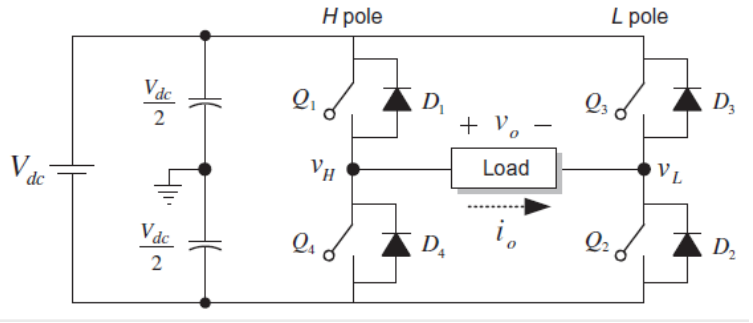

Figure 5 Full Bridge Inverter [11]

Table 1 Switching States and Output Voltages [11]

Switch State	Pole Voltage		Load Voltage
	v_H	v_L	$v_o = v_H - v_L$
Q_1, Q_2 On	$\frac{V_{dc}}{2}$	$-\frac{V_{dc}}{2}$	V_{dc}
Q_4, Q_3 On	$-\frac{V_{dc}}{2}$	$\frac{V_{dc}}{2}$	$-V_{dc}$
Q_1, Q_3 On	$\frac{V_{dc}}{2}$	$\frac{V_{dc}}{2}$	0
Q_4, Q_2 On	$-\frac{V_{dc}}{2}$	$-\frac{V_{dc}}{2}$	0

The load voltage of this inverter is a square wave which constitutes of a fundamental and harmonics.

$$V_o = \frac{4Vdc}{\pi} \sum_{n=1,3,5\ldots}^{\infty} \frac{\sin nwt}{n} \qquad (2 - 3)$$

However, the inverter can provide 90% of the supply voltage to the load:

$$V_{o,rms} = \frac{1}{\sqrt{2}} \frac{4Vdc}{\pi} = 0.9\ V_{dc} \qquad (2 - 4)$$

2.1.2 Three Phase Inverters

The three-phase inverter consists of three poles. Each pole is switched independently of each other, and the two switches in each pole are alternately switched in 180 degrees intervals. Moreover, to produce three phase voltages, each pole should be placed 120 degrees from the other one.

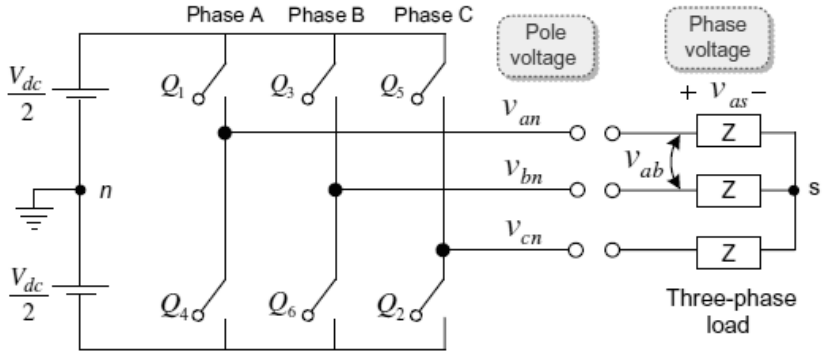

Figure 6 Three Phase Inverter Circuit [11]

The phase and line voltages will be defined based on the states of the switches. There are only 8 possible combinations. These results are summarized in the table below:

Switch States			Pole Voltages			Phase Voltages		
S_a	S_b	S_c	v_{an}	v_{bn}	v_{cn}	v_{as}	v_{bs}	v_{cs}
0	0	0	$-\frac{1}{2}V_{dc}$	$-\frac{1}{2}V_{dc}$	$-\frac{1}{2}V_{dc}$	0	0	0
0	0	1	$-\frac{1}{2}V_{dc}$	$-\frac{1}{2}V_{dc}$	$\frac{1}{2}V_{dc}$	$-\frac{1}{3}V_{dc}$	$-\frac{1}{3}V_{dc}$	$\frac{2}{3}V_{dc}$
0	1	0	$-\frac{1}{2}V_{dc}$	$\frac{1}{2}V_{dc}$	$-\frac{1}{2}V_{dc}$	$-\frac{1}{3}V_{dc}$	$\frac{2}{3}V_{dc}$	$-\frac{1}{3}V_{dc}$
0	1	1	$-\frac{1}{2}V_{dc}$	$\frac{1}{2}V_{dc}$	$\frac{1}{2}V_{dc}$	$-\frac{2}{3}V_{dc}$	$\frac{1}{3}V_{dc}$	$\frac{1}{3}V_{dc}$
1	0	0	$\frac{1}{2}V_{dc}$	$-\frac{1}{2}V_{dc}$	$-\frac{1}{2}V_{dc}$	$\frac{2}{3}V_{dc}$	$-\frac{1}{3}V_{dc}$	$-\frac{1}{3}V_{dc}$
1	0	1	$\frac{1}{2}V_{dc}$	$-\frac{1}{2}V_{dc}$	$\frac{1}{2}V_{dc}$	$\frac{1}{3}V_{dc}$	$-\frac{2}{3}V_{dc}$	$\frac{1}{3}V_{dc}$
1	1	0	$\frac{1}{2}V_{dc}$	$\frac{1}{2}V_{dc}$	$-\frac{1}{2}V_{dc}$	$\frac{1}{3}V_{dc}$	$\frac{1}{3}V_{dc}$	$-\frac{2}{3}V_{dc}$
1	1	1	$\frac{1}{2}V_{dc}$	$\frac{1}{2}V_{dc}$	$\frac{1}{2}V_{dc}$	0	0	0

Figure 7 Phase and Line Voltages of Three Phase Inverters [11]

Based on these combinations, the phase voltages can be traced. Alternatively, the line voltages can be obtained by obtaining the voltage difference between any two-phase voltages, i.e., $V_{ab} = V_a - V_b$.

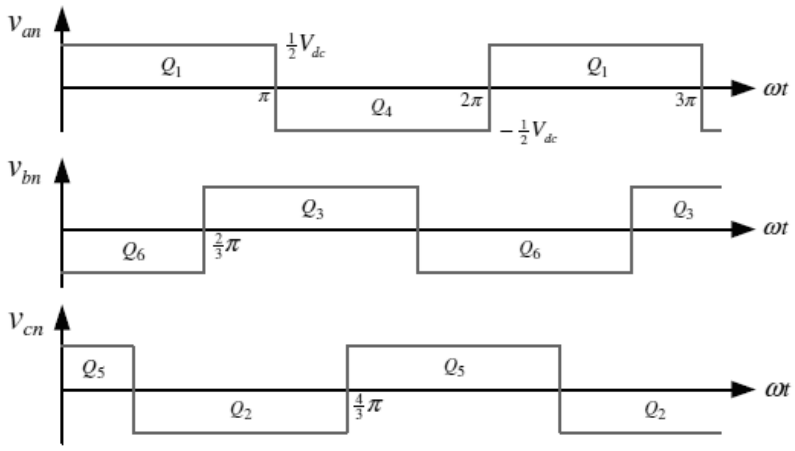

Figure 8 Three Phase Inverter Phase Voltages [11]

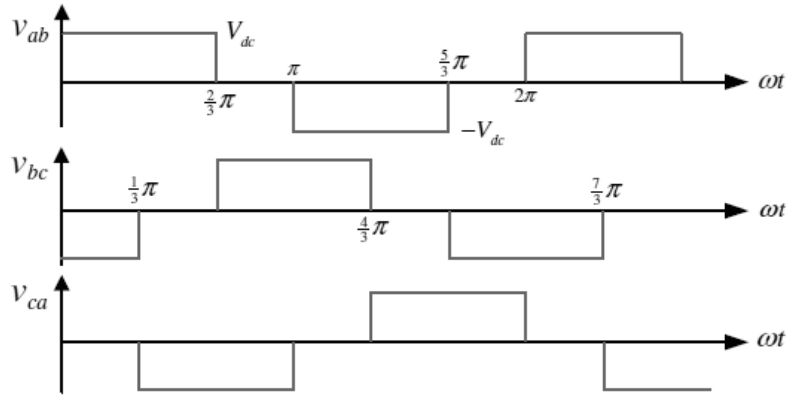

Figure 9 Three Phase Inverter Line to Line Voltages [11]

This inverter is known by six-step inverter due to the shape of its output load voltages. Like the previous inverters, its phase voltages are expressed in term of Fourier series as:

$$V_{an} = \frac{2Vdc}{\pi} \sum_{n=1,3,5\ldots}^{\infty} \frac{\sin nwt}{n} \quad (2 - 5)$$

$$V_{bn} = \frac{2Vdc}{\pi} \sum_{n=1,3,5\ldots}^{\infty} \frac{\sin[n(wt-120°)]}{n} \quad (2 - 6)$$

$$V_{cn} = \frac{2Vdc}{\pi} \sum_{n=1,3,5\ldots}^{\infty} \frac{\sin[n(wt+120°)]}{n} \quad (2 - 7)$$

Moreover, the line voltages will follow the same form. For example, $V_{ab} = V_{an} - V_{bn}$ will be:

$$V_{ab} = \frac{4Vdc}{\pi} \sum_{n=1,3,5\ldots}^{\infty} \cos\frac{n\pi}{6} \sin n \left(wt + \frac{\pi}{6}\right) \quad (2 - 8)$$

Then, upon expansion, V_{ab} will be equivalent to $\frac{2\sqrt{3}Vdc}{\pi} \left[\sin\left(wt + \frac{\pi}{6}\right) - \frac{1}{5}\sin 5\left(wt + \frac{\pi}{6}\right) - \frac{1}{7}\sin 7\left(wt + \frac{\pi}{6}\right) + \frac{1}{11}\sin 11\left(wt + \frac{\pi}{6}\right) + \frac{1}{13}\sin 13\left(wt + \frac{\pi}{6}\right) + \cdots\right.$

Since the line to line voltages are the difference between two phase voltages, they are expected not to have any harmonics which is a multiple of three. That due to the fact that each phase is ahead from the other one by 120 degrees, which means harmonics of multiples of three will be in phase with each other, and eventually cancelling each other.

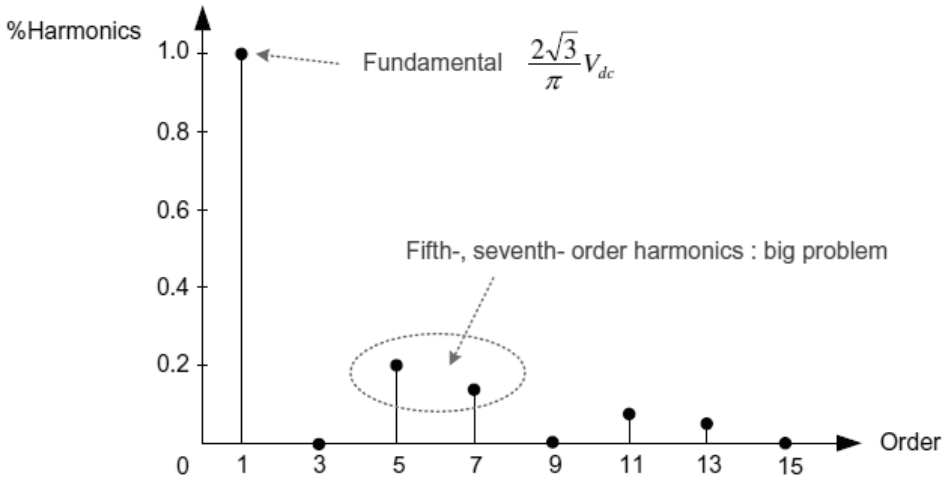

Figure 10 Harmonics Spectrum in Line to Line Voltages [11]

Eventually, the prospective output of phase voltage of the of this inverter at the level of the load would be in the six-step pattern. However, the current is expected not to follow that pattern, due to the frequent presence of inductive loads, which entail charging and discharging cycles.

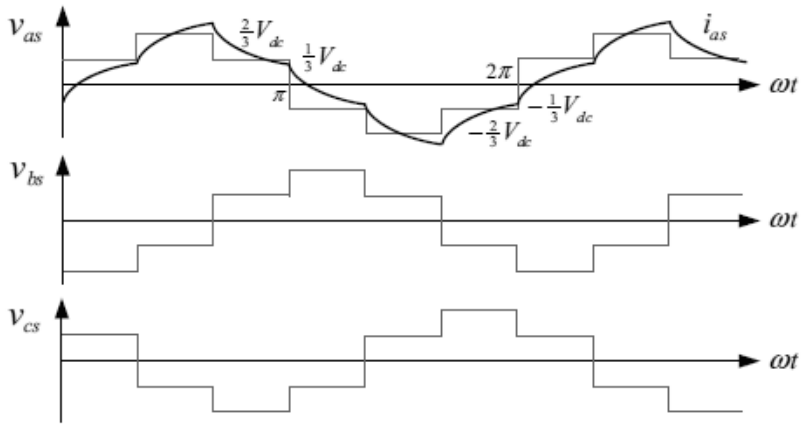

Figure 11 Load Phase Voltage and Current Output [11]

2.2 Modulation Techniques

Pulse width modulation is a technique that compares a pulsating waveform with another controlled input signal to form certain duty cycle. The duty cycle, or the percentage of the time switch is active, governs the output signal. This is determined by the intersections of the reference voltage waveform and the carrier waveform giving the opening and closing time of the switches.

PWM is prevalent in various applications related to motor speed control, converters and amplifiers. It affects the efficiency of power electronics in a way that will lead to reduce the total power delivered to a load without losses, instead of employing resistive loads to limit the current. PWM technique adjusts the voltage applied to a motor by varying the duty cycle, and that causes a speed change at the motor terminals. The higher the ratio of closed to opened switch, the higher the higher the power delivered to the load is. When the transition of the switch from ON to OFF and vice versa is fast, the average power dissipated is low compared to the delivered power. PWM amplifiers are smaller and more efficient than linear power amplifiers, which delivers power continuously rather than pulsating. [12]

Many PWM methods are involved in industrial applications like in solid state devices and advanced microprocessors. But no single technique is exemplary to every application. In fact, diligent research has been made in that area since the 1970s. These PWM drives can control both the frequency and the voltage applied to the motor. The implemented strategies and control schemes play a decisive role in minimizing harmonics and switching losses in inverters. The first modulation techniques were developed in 1960s by Kirnnich, Heinrick and Bowes. The current focus is to create innovative schemes capable of producing a maximum fundamental component with minimum harmonics.

The carrier based PWM techniques were the first and most wide used ones in most applications. The sinusoidal PWM technique was one of the earliest schemes of the carrier-based mode, involving the comparison of a carrier signal and a pure sinusoidal signal. It was first introduced by Stimmler in 1964. The main defect of the SPWM is its low utilization rate of DC voltage (78.5%), compared to 100% of the six-step wave technique. At that time, research was concentrated at improving that utilization rate.

The next major development in soothing the under-utilization problem was introduced by Buja, in 1975. He introduced the third harmonic injection pulse width modulation (THIPWM). He added a third harmonic signal to the pure sinusoidal reference, boosting the utilization DC voltage rate by 15.5%.

The next advance in increasing the voltage was by the space vector PWM (SVPWM) technique. This method was introduced in the 1980s and improved by Broeck in 1988. Compared to the third harmonic injection technique, they both have similar results, but their implementation is different. The SVPWM is dominates among other techniques in three phase inverters applications, due to its lower switching losses, reduced harmonics and acceptable utilized voltage output.

When comparing the SVPWM to SPWM, the first outperforms the second technique evidently, in terms of reduced harmonics and higher efficiency. In fact, the maximum peak of the SVPWM technique is 90.6% of the inverter ability. In comparison with the traditional sinusoidal modulation, this resembles a 15.5% increase in the maximum voltage output.[12]

Based on the SVPWM technique, many other schemes had popped out. One of them is the over modulation of SVPWM which separated the over modulation range into two modes of operation and increased the utilization rate of DC voltage. Other schemes include the

discontinuous SVPWM techniques which involves turning a switch off repeatedly over a determined portion of a sector of the signal.

2.2.1 Sinusoidal Pulse Width Modulation (SPWM)

2.2.1.1 SPWM Concept

The sinusoidal PWM technique generates sinusoidal signals by the filtration of pulse waveform with variable width. A higher switching frequency will lead to a cleaner filtered sinusoidal form. The required voltage output will be obtained by varying the frequency and amplitude of a reference or modulating voltage. Those variations would alter the pulse width-patterns of a sinusoidal modulated output voltage.[12]

To obtain the signals, a low-frequency sinusoidal waveform is compared with a high-frequency triangular waveform, which represents the carrier waveform. The switching state is changed when the sine wave intersects the triangular wave. The positions of crossing specify the variable switching time between the between the two alternating states.

In three phase SPWM, a triangular wave (V_t) will be compared by a set of three sinusoidal control voltages (V_a,V_b, and V_c), which are out of phase with each other by 120 degrees. The prospect levels of the waveforms' intersections are used to control the switching state of the switches in each leg of the inverter.

A six-step inverter is made up of six switches named S_1 to S_6. Each phase output is connected to the middle of each inverter leg. The output comparators create the control signals for the set of three legs of the inverter. Each phase is governed by two switches operating in a complementary mode. This means when a switch is open, the latter should be closed. This will

insure the absence of any short circuit fault. The output phase voltages (V_{a0},V_{b0}, and V_{c0}) of the inverter oscillate between $-V_{dc}/2$ and $+V_{dc}/2$ where V_{dc} is the total DC voltage of the battery.

That means that the peak of the sine waveform is usually less than the peak of the triangular carrier waveform. When the sinusoidal waveform is bigger than the triangular waveform, the upper switch is turned on and the lower switch is turned off. In the same way, if the sinusoidal waveform is smaller than the triangular waveform, the upper switch is turned off and the lower switch is turned on. Depending on these alternating switching states, either the positive or the negative have DC voltage will be applied to the phase output. The switches are governed in pairs ((S_1,S_4), (S_3, S_6), and (S_5,S_2)) and the logic behind these switching control signals is:

- S_1 is ON when $V_a > V_t$ & S_4 is ON when $V_a < V_t$
- S_3 is ON when $V_b > V_t$ & S_6 is ON when $V_b < V_t$
- S_5 is ON when $V_a > V_t$ & S_2 is ON when $V_c < V_t$

Then the pulses width depends on the intersection of the triangular and sinusoidal waveforms. The inverter output voltage (V_{a0}, Vb_0, or V_{c0}) is equal to $+V_{dc}/2$ if V_a,V_b, or V_c is greater than V_t. Similarly, the inverter output voltage (V_{a0}, Vb_0, or V_{c0}) is equal to $-V_{dc}/2$ if V_a,V_b, or V_c is less than V_t. The line to line voltages are obtained from the phase voltages as:

- $V_{ab}= V_{a0}-V_{b0}$
- $V_{bc}= V_{b0}-V_{c0}$
- $V_{ca}= V_{c0}-V_{a0}$

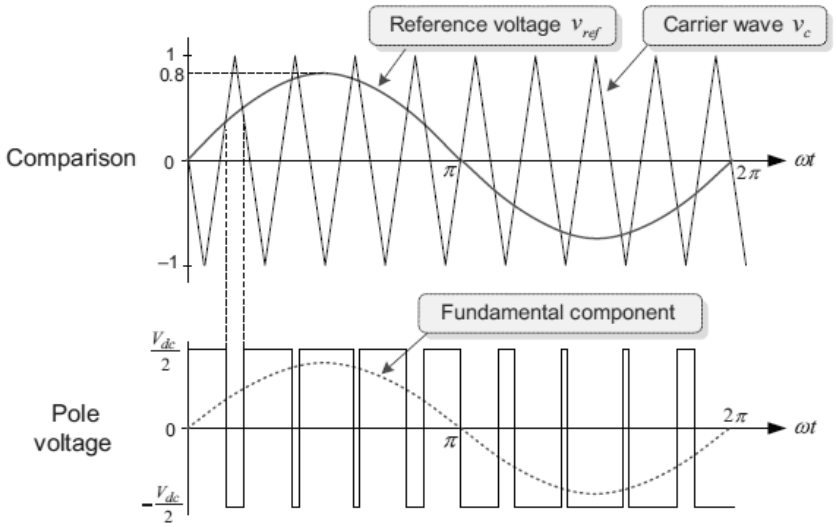

Figure 12 Pulse Width Modulation Comparison [11]

2.2.1.2 Modulation Index of SPWM

As per Fourier series expansion of a symmetrical square wave voltage whose peak value is $V_{dc}/2$, the fundamental magnitude is $2V_{dc}/\pi$. That due to the fact that the maximum of the output voltage resulting from the SPWM method is $V_{dc}/2$. The modulation index (MI) is the ratio of the magnitude of the output voltage generated by SPWM to the fundamental peak value of the maximum square wave. Therefore, the modulation index of the SPWM technique is:

$$MI = \frac{Vpwm}{Vmax} = \frac{\frac{Vdc}{2}}{\frac{2Vdc}{\pi}} = \frac{\pi}{4} = 78.5\% \qquad (2 - 9)$$

2.2.2 Third Harmonic Sinusoidal Pulse Width Modulation

2.2.2.1 Concept and Derivation

The SPWM is the simplest modulation scheme but it is not capable of fully utilizing the available DC bus voltage supply. To reduce this problem, a third harmonic injection technique to the sinusoidal waveform is applied to improve the performance of the inverter. Consider a waveform constituting of a fundamental component and a triple frequency term:[12]

$$y = \sin\theta + A \sin 3\theta \qquad (2 - 10)$$

where $\theta = \omega t$ and A is a parameter to be optimized while keeping the amplitude of y under unity. The maximum value of y is set by performing the derivative of y with respect to θ equalized to zero. Then,

$$\frac{dy}{d\theta} = \cos\theta + 3A \cos 3\theta = 0 \qquad (2 - 11)$$

Upon solving this equation using certain trigonometric identities, the peak value of y can be determined by:

$$Y = 8A \left(\frac{1+3A}{12A}\right)\frac{3}{2} \qquad (2 - 12)$$

To determine the optimum value of A for a minimized Y, Y can be differentiated with respect to A and equated to zero,

$$\frac{dY}{dA} = 0 \qquad (2 - 13)$$

then,

$$A = \frac{-1}{3} \text{ or } A = \frac{1}{6}. \qquad (2 - 14)$$

The negative value of A would make the value of Y greater than unity. Hence, $A = \frac{1}{6}$.

Also,

$$y = \sin\theta + \frac{1}{6}\sin 3\theta. \qquad (2 - 15)$$

It should be noted that all triple harmonics are eliminated by values of $\theta = \frac{n\pi}{3}$. However, the addition of a third harmonic with peak magnitude of one sixth to the modulation waveform has the effect of reducing the peak value by a factor of $\sqrt{3}/2$ without changing the amplitude of the fundamental. It is permitted to increase the amplitude of the modulating waveform by a factor K, so that the full output voltage range will be used. The waveform can be expressed as:

$$y = K(\sin\theta + \frac{1}{6}\sin 3\theta), \qquad (2 - 16)$$

while the value of K is equal to $2/\sqrt{3}$.

Thus, the obtained modulating signals will be,

$$V_{an} = \frac{2}{\sqrt{3}}\left(\sin(wt) + \frac{1}{6}\sin(3wt)\right) \quad (2 - 17)$$

$$V_{bn} = \frac{2}{\sqrt{3}}\left(\sin\left(wt - \frac{2\pi}{3}\right) + \frac{1}{6}\sin(3wt)\right) \quad (2 - 18)$$

$$V_{cn} = \frac{2}{\sqrt{3}}\left(\sin\left(wt + \frac{2\pi}{3}\right) + \frac{1}{6}\sin(3wt)\right) \quad (2 - 19)$$

The addition of this harmonic will produce a 15.5% increase in the amplitude of the fundamental phase voltages. The THIPWM is implemented in the same way as SPWM, where the reference waveforms are compared with a triangular waveform. As a result, the amplitude of the reference waveforms does not exceed the DC supply voltage of $V_{dc}/2$, but the fundamental component is higher than the supply voltage V_{dc}.

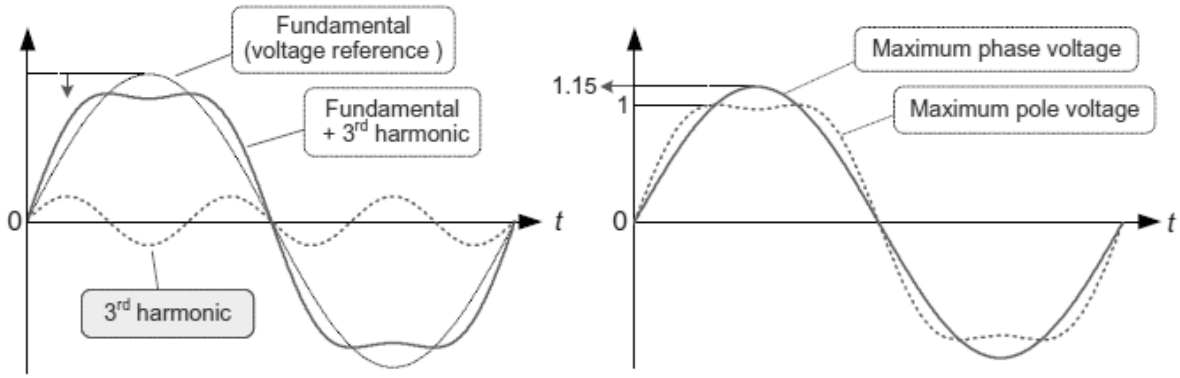

Figure 13 Third Harmonic Injected Waveform

2.2.3 Space Vector Modulation (SVM)

2.2.3.1 Principle of Space Vector Modulation

The circuit of a typical three phase voltage source PWM inverter is shown below. S_1 to S_6 are the 6 switches that shape the inverter output, in which they are controlled by the gating signals. When an upper switch is switched on, i.e., when a, b or c is 1, the corresponding lower switch is turned off, i.e., a', b' or c' is 0. Then, the on and off states of upper switches S1, S3 and S5 can be

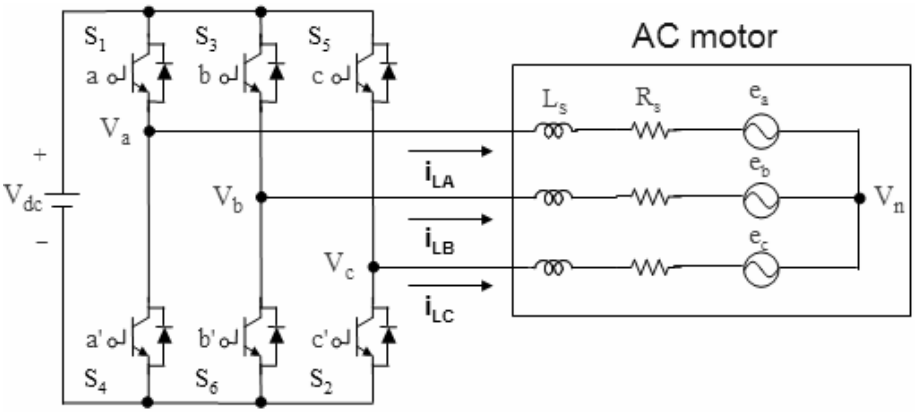

Figure 14 Three-phase voltage source PWM Inverter [13]

used to determine the output voltage. The relationship between the switching variable vector [a, b, c]^t and the line-to-line voltage vector [V_{ab} V_{bc} V_{ca}]^t is given by:

$$\begin{bmatrix} Vab \\ Vbc \\ Vca \end{bmatrix} = V_{dc} \begin{bmatrix} 1 & -1 & 0 \\ 0 & 1 & -1 \\ -1 & 0 & 1 \end{bmatrix} \begin{bmatrix} a \\ b \\ c \end{bmatrix}. \qquad (2 - 20)$$

Then, the relationship between the switching variable vector [a, b, c]^t and the phase voltage vector [V_a V_b V_c]^t can be expressed below:

$$\begin{bmatrix} Van \\ Vbn \\ Vcn \end{bmatrix} = \frac{Vdc}{3} \begin{bmatrix} 2 & -1 & -1 \\ -1 & 2 & -1 \\ -1 & -1 & 2 \end{bmatrix} \begin{bmatrix} a \\ b \\ c \end{bmatrix}. \quad (2 - 21)$$

There are eight possible states of on and off patterns for the three upper power switches. The on and off states of the lower power devices are opposite to the upper one and so are easily determined once the states of the upper power transistors are determined. Then, the eight switching vectors, output line to neutral voltage (phase voltage), and output line-to-line voltages in terms of DC-link V_{dc}, are given in the table below.[13]

Table 2 Switching Vectors, Phase Voltages And Output Line To Line Voltages [13]

Voltage Vectors	Switching Vectors			Line to neutral voltage			Line to line voltage		
	a	b	c	V_{an}	V_{bn}	V_{cn}	V_{ab}	V_{bc}	V_{ca}
V_0	0	0	0	0	0	0	0	0	0
V_1	1	0	0	2/3	-1/3	-1/3	1	0	-1
V_2	1	1	0	1/3	1/3	-2/3	0	1	-1
V_3	0	1	0	-1/3	2/3	-1/3	-1	1	0
V_4	0	1	1	-2/3	1/3	1/3	-1	0	1
V_5	0	0	1	-1/3	-1/3	2/3	0	-1	1
V_6	1	0	1	1/3	-2/3	1/3	1	-1	0
V_7	1	1	1	0	0	0	0	0	0

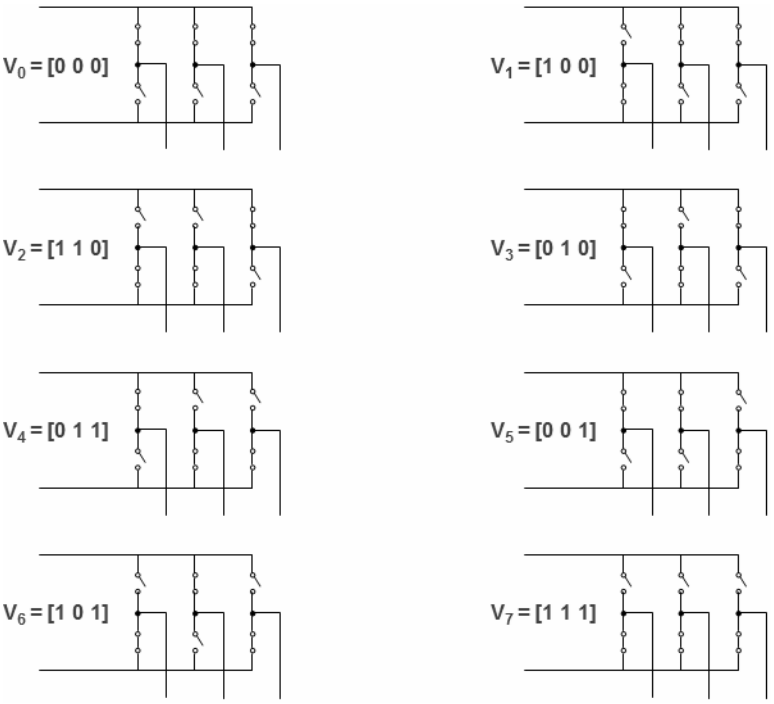

Figure 15 The Eight Inverter Voltage Vectors (V0 To V7) [13]

Space Vector PWM (SVPWM) refers to a special switching sequence of the upper three power transistors of a three-phase power inverter. It has been shown to generate less harmonic distortion in the output voltages and or currents applied to the phases of an AC motor and to provide more efficient use of supply voltage compared to SPWM.

In order to implement the SVPWM, the voltage equations in the *abc* reference frame can be transformed into the stationary *dq* reference frame that is made up of the horizontal (d) and vertical (q) axes as shown below:

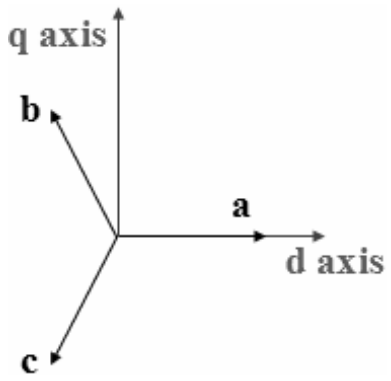

Figure 16 The Relationship of abc Reference Frame and Stationary dq Reference Frame [13]

From the figure above, the relationship between the two reference frames is:

$$f_{dq0} = K_s f_{abc}, \tag{2 - 22}$$

$$\text{where } K_s = \frac{2}{3}\begin{bmatrix} 1 & -1/2 & -1/2 \\ 0 & \sqrt{3}/2 & -\sqrt{3}/2 \\ 1/2 & 1/2 & 1/2 \end{bmatrix}. \tag{2 - 23}$$

This transformation is equivalent to an orthogonal projection of $[a, b, c]^t$ onto the two-dimensional perpendicular to the vector $[1, 1, 1]^t$ (the equivalent d-q plane) in a three-dimensional coordinate system. Then, six non-zero vectors and two zero vectors are possible. Six nonzero vectors (V_1 - V_6) shape the axes of a hexagonal, and feed electric power to the load. The angle between any adjacent two non-zero vectors is 60 degrees. Meanwhile, two zero vectors (V_0 and V_7) are at the origin and apply zero voltage to the load. The eight vectors are called the basic space vectors and are denoted by V_0, V_1, V_2, V_3, V_4, V_5, V_6, and V_7. The same transformation can be applied to the desired output voltage to get the desired reference voltage vector V_{ref} in the d-q plane. [13]

The objective of space vector PWM technique is to approximate the reference voltage vector V_{ref} using the eight switching patterns. One simple method of approximation is to generate the average output of the inverter in a small period, T to be the same as that of V_{ref} in the same period.

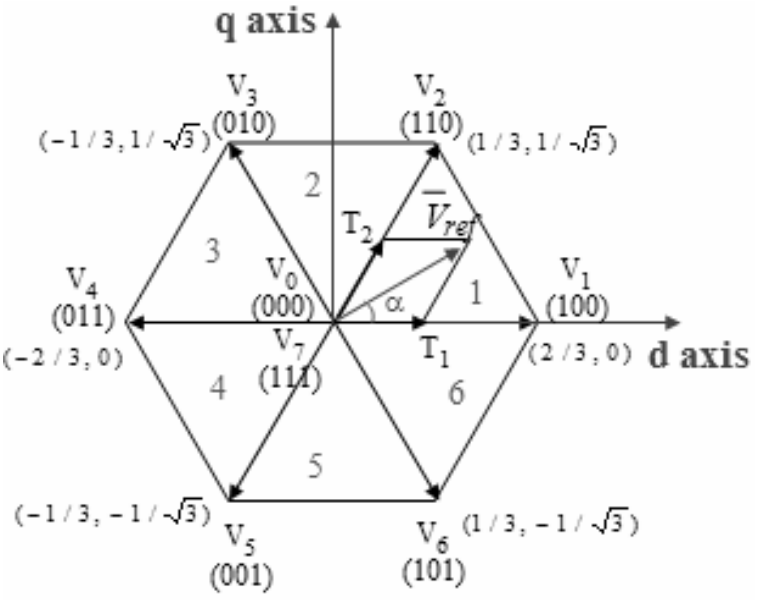

Figure 17 Basic Switching Vectors and Sectors [13]

2.2.3.2 SVM Implementation

Thus, to perform SVM, three steps should be done:

1- Determining V_d, V_q, V_{ref} and angle (α).

2- Determining the time intervals T_1, T_2 and T_0.

3- Determining the switching time for all switches (S_1 to S_6).

2.2.3.2.1 Step 1: Determining V_d, V_q, V_{ref} and angle (α)

V_d, V_q, V_{ref} and angle (α) can be determined as follows:

- $V_d = V_{an} - V_{bn}.\cos(60) - V_{cn}.\cos(60) = V_{an} - \frac{1}{2}V_{bn} - \frac{1}{2}V_{cn}$
- $V_q = 0 + V_{bn}.\cos(30) - V_{cn}.\cos(30) = V_{an} + \frac{\sqrt{3}}{2}V_{bn} - \frac{\sqrt{3}}{2}V_{cn}$

$$\text{Then, } \begin{bmatrix} V_d \\ V_q \end{bmatrix} = \frac{2}{3}\begin{bmatrix} 1 & -\frac{1}{2} & -\frac{1}{2} \\ 0 & \frac{\sqrt{3}}{2} & -\frac{\sqrt{3}}{2} \end{bmatrix}\begin{bmatrix} V_{an} \\ V_{bn} \\ V_{cn} \end{bmatrix}. \quad (2 - 24)$$

And,

$$|V_{ref}| = \sqrt{V_d^2 + V_q^2} \quad (2 - 25)$$

$$\alpha = \tan^{-1}\frac{V_q}{V_d} = 2\pi f t \quad (2 - 26)$$

The figure below shows a sample transformation of the voltage reference from the abc system to dq0 system in terms of V_d, V_q and α.

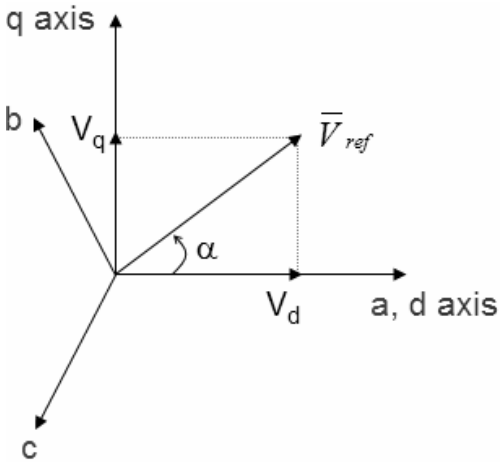

Figure 18 Voltage Space Vector and its Components in dq System [13]

2.2.3.2.2 Step 2: Determining the time intervals T_1, T_2 and T_0

The switching time duration at Sector 1 can be calculated as follows:

$$\int_0^{Tz} V_{ref} = \int_0^{T1} V_1\, dt + \int_{T_1}^{T_1+T_2} V_2\, dt + \int_{T_1+T_2}^{Tz} V_0 \qquad (2 - 27)$$

Then,

$$T_z.\left|V_{ref}\right|.\begin{bmatrix}\cos\alpha\\ \sin\alpha\end{bmatrix} = T_1.\frac{2}{3}.V_{dc}.\begin{bmatrix}1\\0\end{bmatrix} + T_2.\frac{2}{3}.V_{dc}.\begin{bmatrix}\cos\frac{\pi}{3}\\ \sin\frac{\pi}{3}\end{bmatrix} \qquad (2 - 28)$$

Therefore,

$$T_1 = T_z.a.\frac{\sin\frac{\pi}{3} - \alpha}{\sin\frac{\pi}{3}} \qquad (2 - 29)$$

$$T_2 = T_z.a.\frac{\sin\alpha}{\sin\frac{\pi}{3}} \qquad (2 - 30)$$

$$T_0 = T_z - T_1 - T_2 \qquad (2 - 31)$$

Where $T_z = \frac{1}{f_z}$ and $a = \frac{|V_{ref}|}{\frac{2}{3}.V_{dc}}$.

The switching times in any sector are:

$$T_1 = \frac{\sqrt{3}\,.Tz\,.|Vref|}{Vdc}\left(\sin\frac{n}{3}\pi\cos\alpha - \cos\frac{n}{3}\pi\sin\alpha\right) \quad (2 - 32)$$

$$T_2 = \frac{\sqrt{3}\,.Tz\,.|Vref|}{Vdc}\left(-\sin\frac{n-1}{3}\pi\cos\alpha + \cos\frac{n-1}{3}\pi\sin\alpha\right) \quad (2 - 33)$$

$$T_0 = Tz - T_1 - T_2 \quad (2 - 34)$$

Where n =1 through 6 and $0 \leq \alpha \leq 60°$.

The figure below shows a sample of the voltage reference in sector 1 being formed by the associated voltages and switching times.

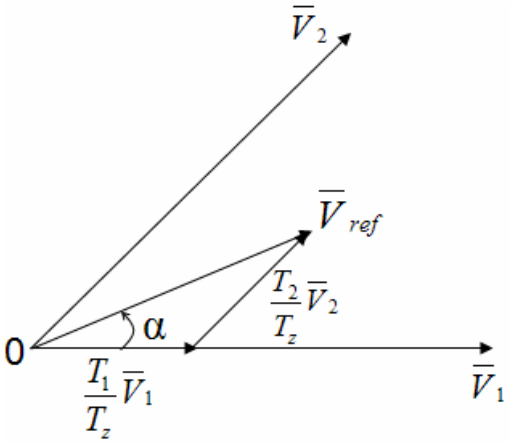

Figure 19 Reference Vector in Sector 1 [13]

2.2.3.2.3 Step 3: Determining the switching time for all switches (S_1 to S_6)

The SVM switching patterns at each sector will be presented below.

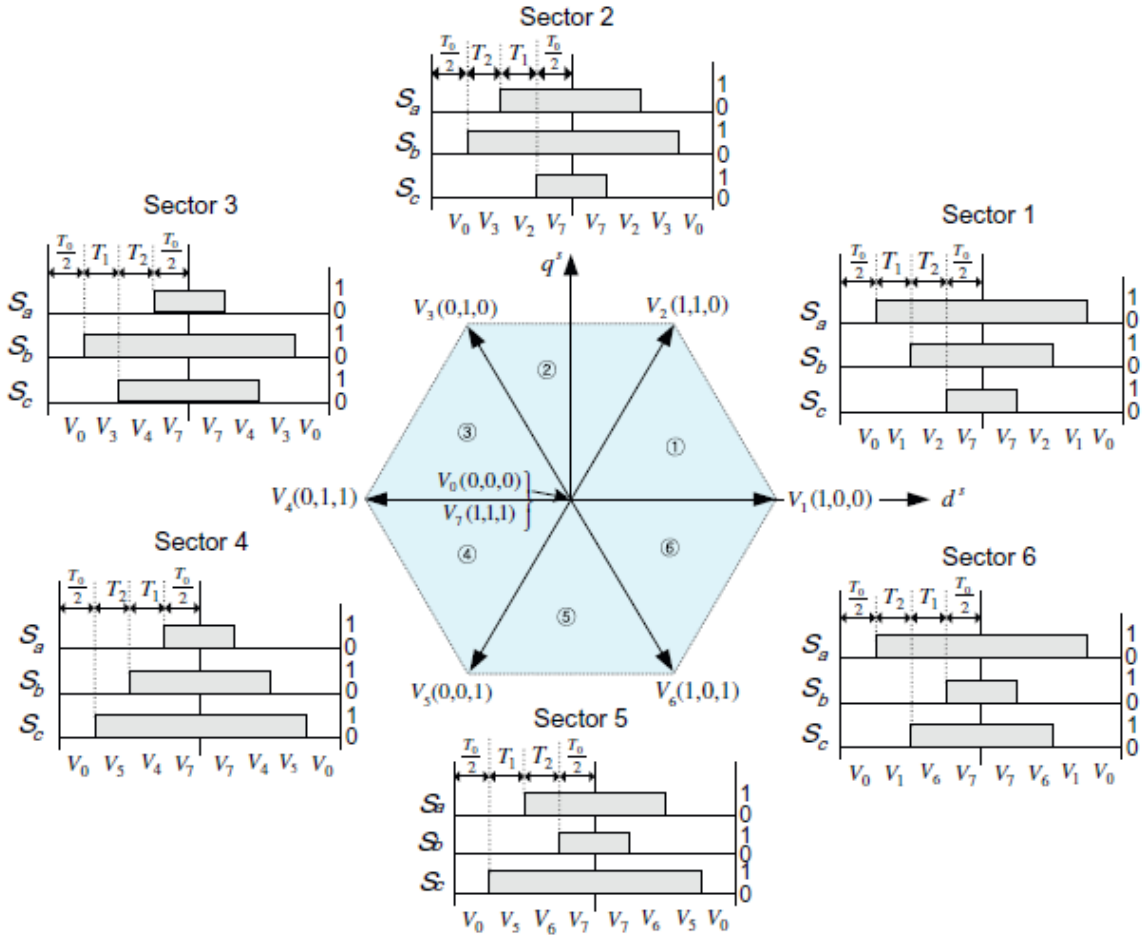

Figure 20 Switching Times of Each Sector [11]

Based on the switching patterns above, the switching times for all switches will be presented below and used to implement SVM in Simulink.

Table 3 Switching Times at Each Sector [13]

Sector	Upper Switches (S_1, S_3, S_5)	Lower Switches (S_4, S_6, S_2)
1	$S_1 = T_1 + T_2 + T_0/2$ $S_3 = T_2 + T_0/2$ $S_5 = T_0/2$	$S_4 = T_0/2$ $S_6 = T_1 + T_0/2$ $S_2 = T_1+T_2+T_0/2$
2	$S_1 = T_1 + T_0/2$ $S_3 = T_1 + T_2 + T_0/2$ $S_5 = T_0/2$	$S_4 = T_2 + T_0/2$ $S_6 = T_0/2$ $S_2 = T_1+T_2+T_0/2$
3	$S_1 = T_0/2$ $S_3 = T_1 + T_2 + T_0/2$ $S_5 = T_2 + T_0/2$	$S_4 = T_1+T_2+T_0/2$ $S_6 = T_0/2$ $S_2 = T_1 + T_0/2$
4	$S_1 = T_0/2$ $S_3 = T_1 + T_0/2$ $S_5 = T_1 + T_2 + T_0/2$	$S_4 = T_1+T_2+T_0/2$ $S_6 = T_2 + T_0/2$ $S_2 = T_0/2$
5	$S_1 = T_2 + T_0/2$ $S_3 = T_0/2$ $S_5 = T_1 + T_2 + T_0/2$	$S_4 = T_1 + T_0/2$ $S_6 = T_1+T_2+T_0/2$ $S_2 = T_0/2$
6	$S_1 = T_1 + T_2 + T_0/2$ $S_3 = T_0/2$ $S_5 = T_1 + T_0/2$	$S_4 = T_0/2$ $S_6 = T_1+T_2+T_0/2$ $S_2 = T_2 + T_0/2$

The table above summarizes the switching times of all switches in the 6 sectors in terms of T_0, T_1 and T_2.

3.0 Model

This section provides an overview of the proposed and tested dual inverter drive through this study.

3.1.1 Schematics

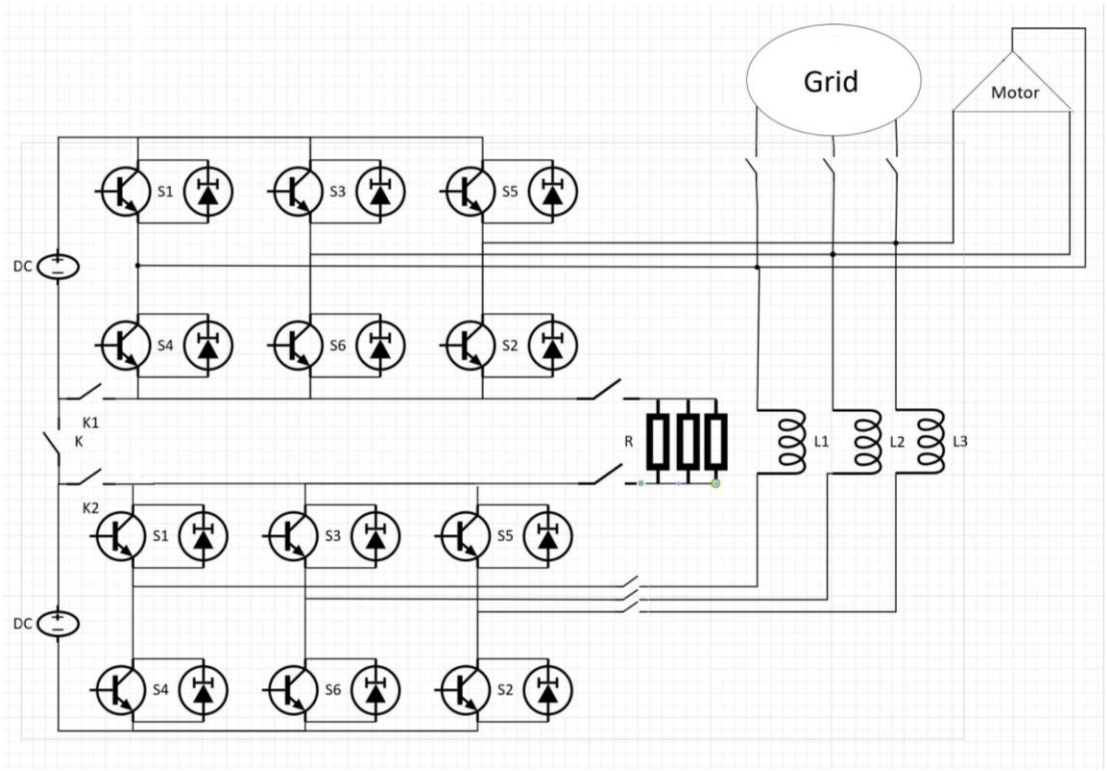

Figure 21 Visio Model of the Tested Dual Inverter Drive

3.1.2 Parameters

Table 4 Model Parameters

Parameter	Value	Unit
AC Grid Reactance	800*10-6	H
AC Grid Voltage	1000	V
Grid Frequency	50	Hz
Nominal Voltage of Batteries	100	V
Leakage Inductance of Motors/Loads	471*10-6	H
Resistance of Motor Winding	0.3	Ohm
Equivalent ‘Sink’ Resistance	0.03	Ohm

3.1.3 Switches

Table 5 Switching States

SPST Switch/Case	K	K1	K2
1	0	0	0
2	0	0	1
3	0	1	0
4	0	1	1
5	1	0	0
6	1	1	0
7	1	0	1
8	1	1	1

Since the are 3 switches in the circuit, 8 combinations of switching states are present. However, not every switching state is applicable. Some switching combinations will lead to open circuit or short circuit operation. These combinations are avoided in the study.

Table 6 Relays States

Relays Element	Relaying State	Reasoning
Grid	0	Disconnect Grid
	1	Connect Grid
Resistance Sink	0	Disconnect Sink
	1	Connect Sink
Open Winding Load	0	Disconnect Load
	1	Connect Load

In comparison with the switching, those 3 relays in the circuit are much less functional. They are present just to connect loads, resistances or grid. They do not alter the inverter status. They tackle the loading of the circuit.

3.1.4 Cases

The four cases of operation are studied in section 4.1.2.6:

- Single inverter operation
- Dual inverter operation
- Dual inverter operation with grid
- Grid only operation

3.1.5 Constraints

The major constraints are:

- Switches voltage and current ratings: this is a usual concern for semiconductor materials in areas of power electronics when they are part of circuits involving power flow with grid.
- Grid size over circuit: This might be overwhelming condition on the performance of small circuit with 2 loads as the one described below. The grid connection would appear as a fault state for the circuit due to the large circulating current.

4.0 Simulations

4.1.1 Three Phase Inverter

This section aims to test a regular three phase inverter in single operation before performing the dual inverter testing.

4.1.1.1 Parameters

- V_{dc}: 100 V
- Load Resistance: 1 Ω
- Carrier Frequency: 5000 Hz
- Modulating Waveform Frequency: 50 Hz
- Modulating Waveform Amplitude: 1
- Third Harmonic Amplitude: 1/6
- Third Harmonic Frequency: 150 Hz

4.1.1.2 Schematics

This Simulink model shows the respective model of the three-phase inverter. The terminals are connected to a three-phase resistance through a three-phase voltage measurement. This model will be used throughout all the simulations.

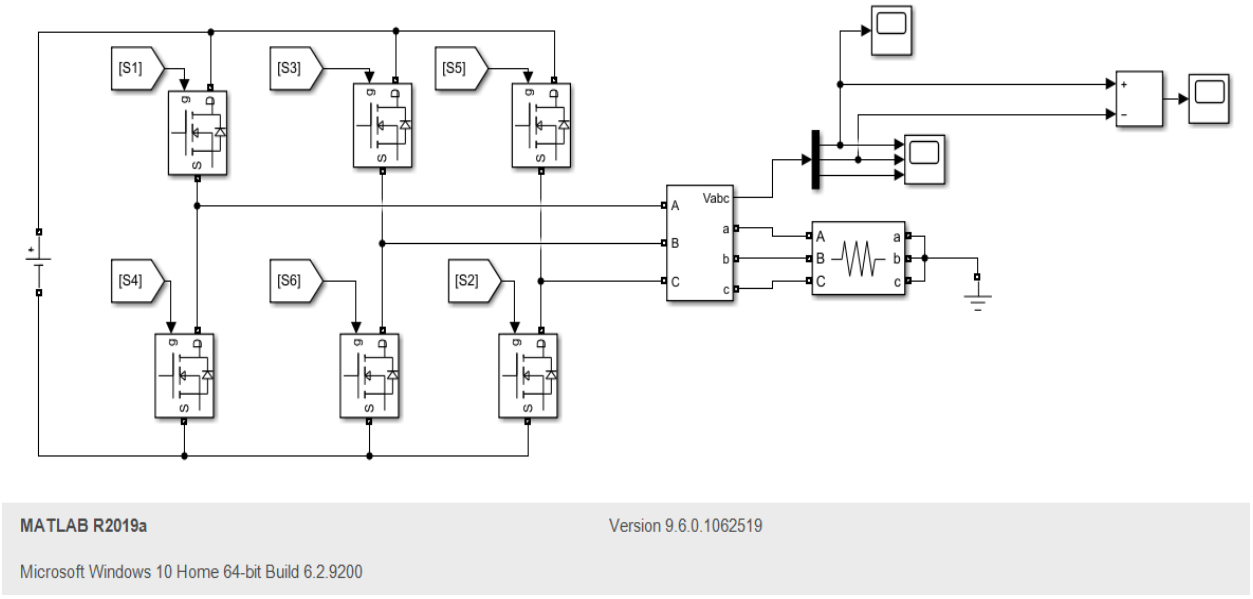

Figure 22 Three Phase Inverter

4.1.1.3 Techniques

4.1.1.3.1 Sinusoidal Pulse Width Modulation

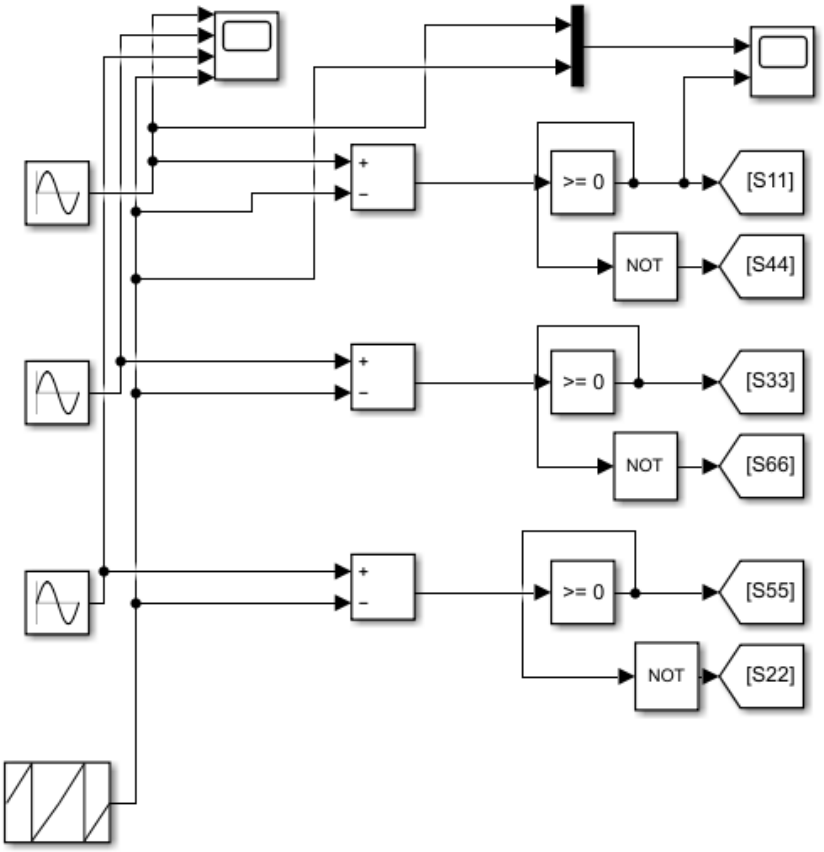

Figure 23 Control Circuit

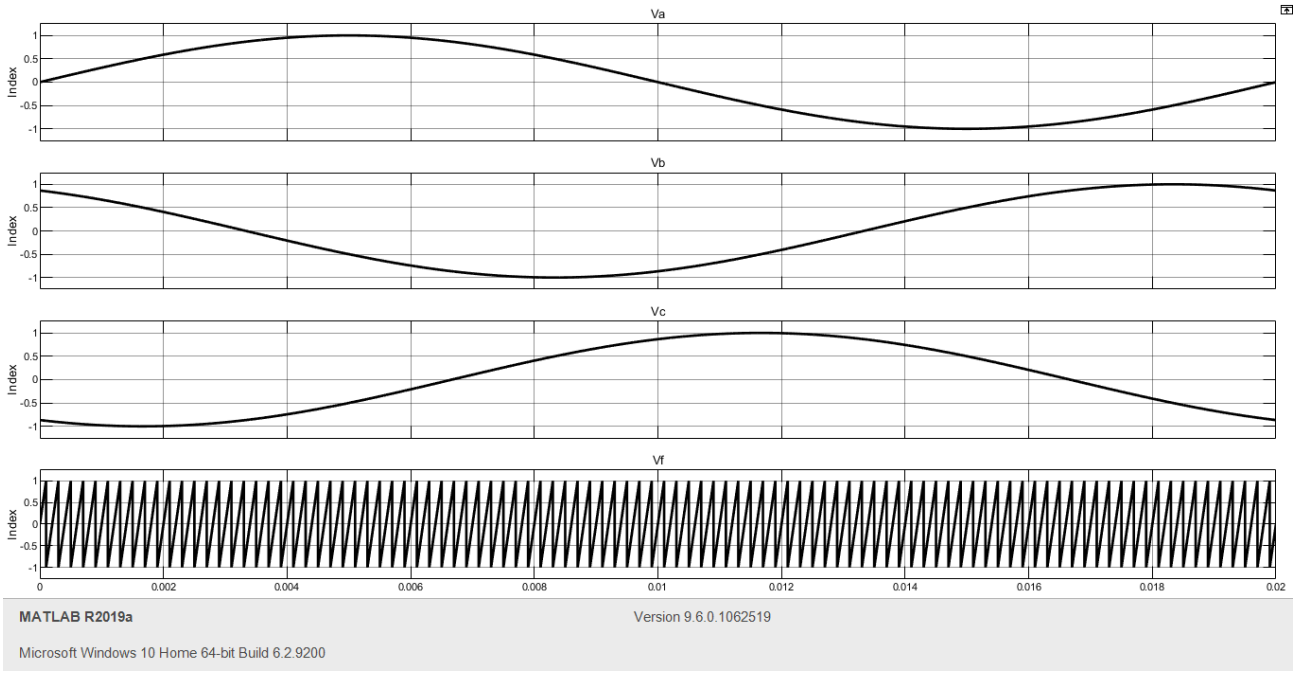

Figure 24 Modulation Signals with Carrier Frequency

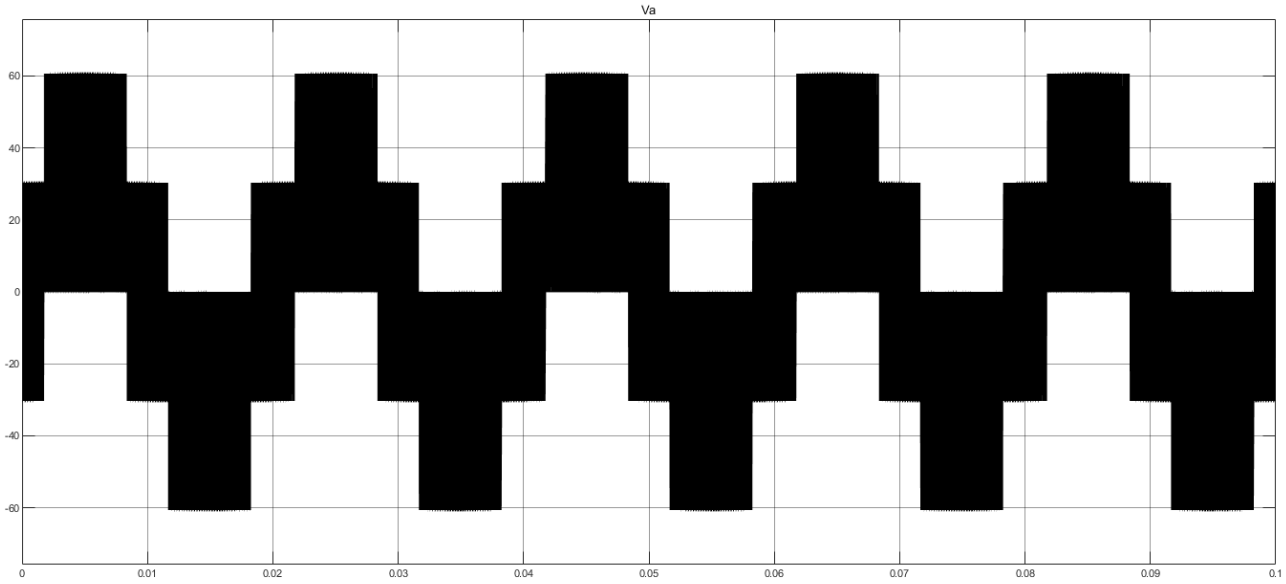

Figure 25 Phase Voltage Output (Va)

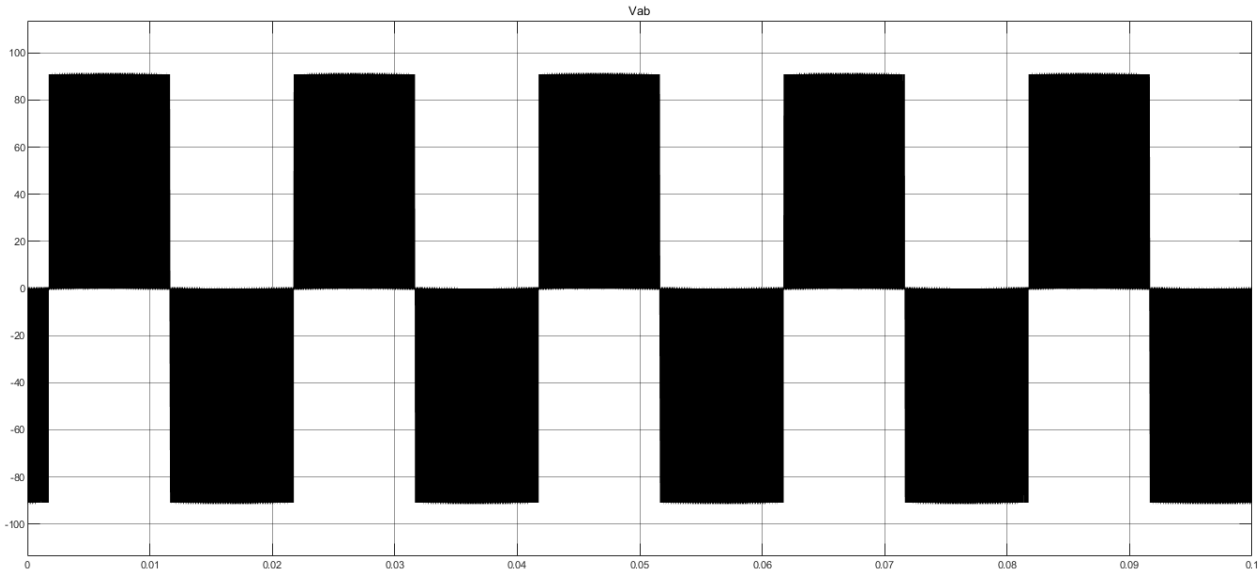

Figure 26 Line Voltage Output (Vab)

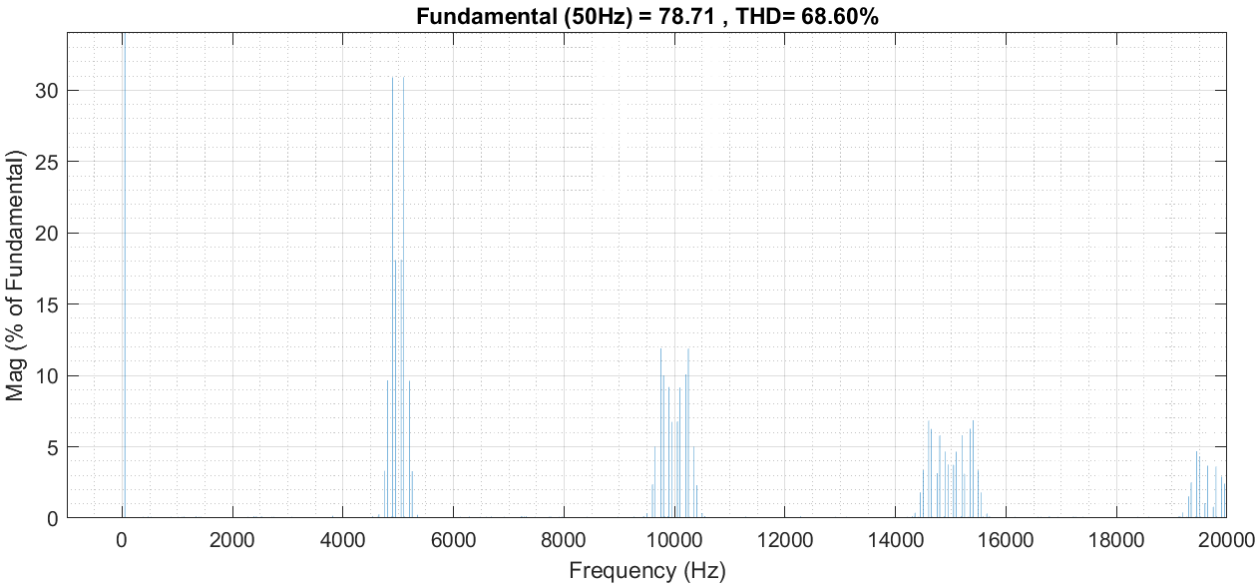

Figure 27 Va Harmonic Spectrum

The results are similar to the values of the equations in 2.0.

4.1.1.3.2 Third Harmonic Sinusoidal Pulse Width Modulation

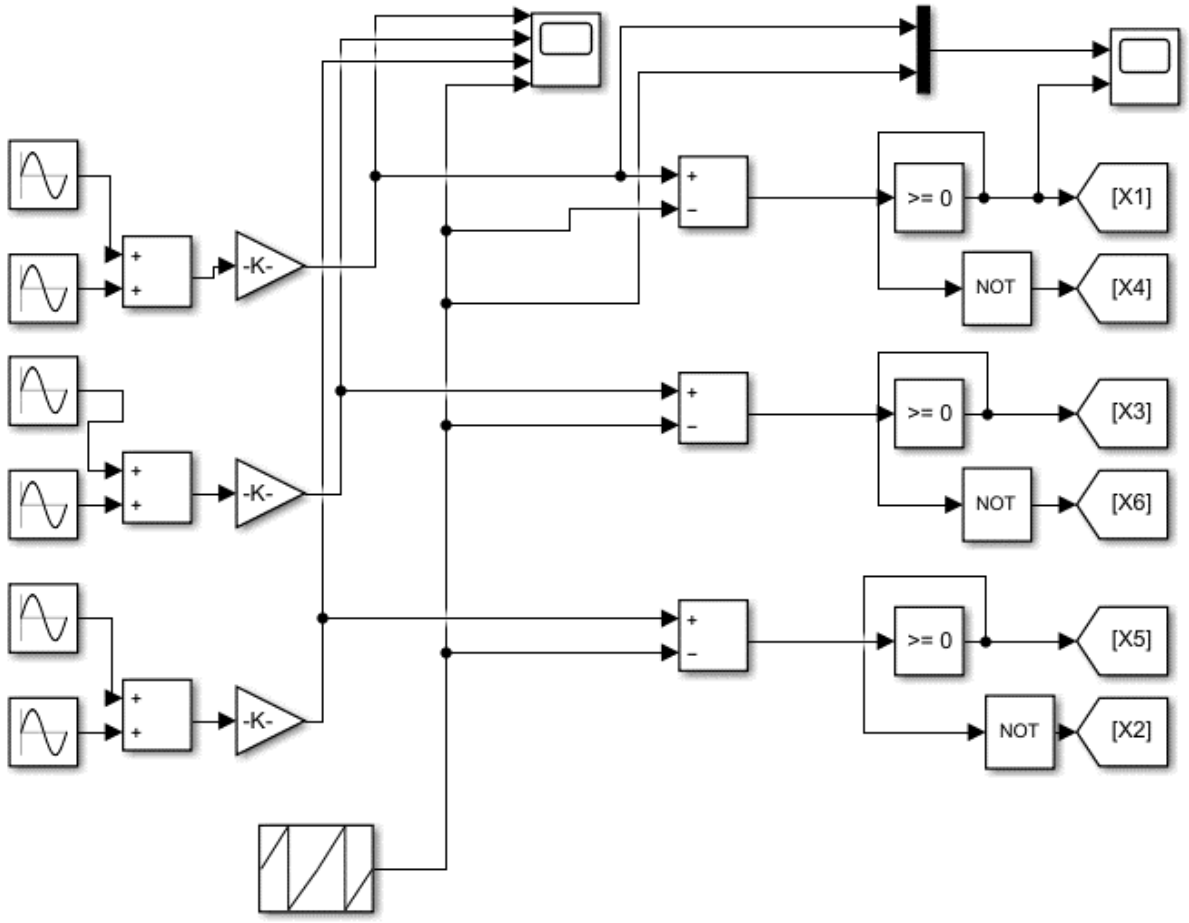

Figure 28 Control Circuit

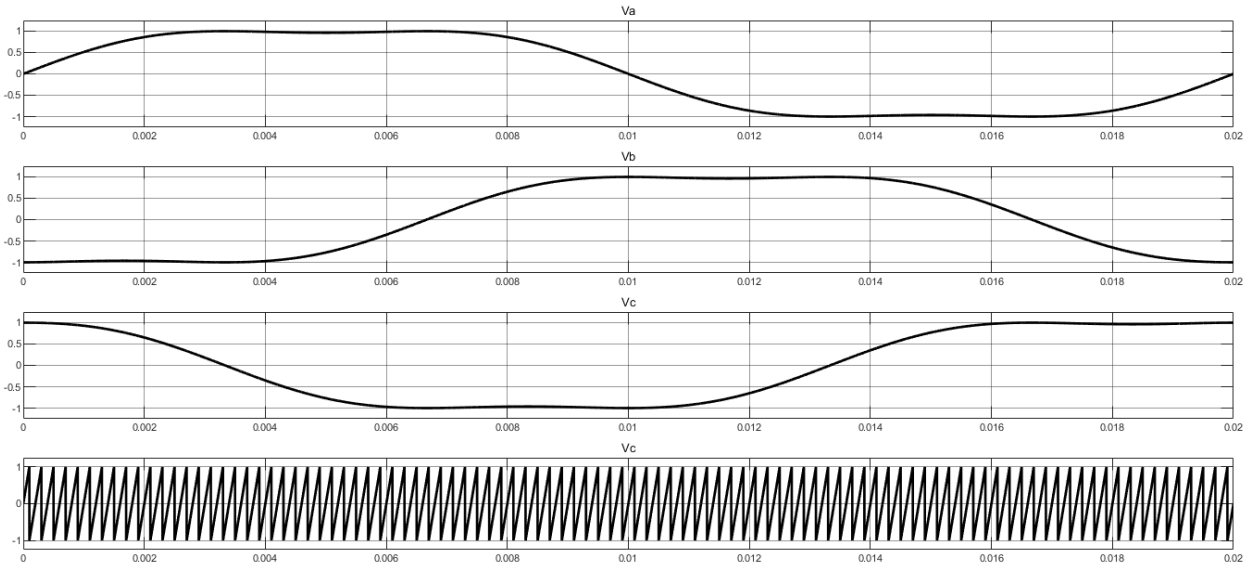

Figure 29 Modulation Signals with Carrier Frequency

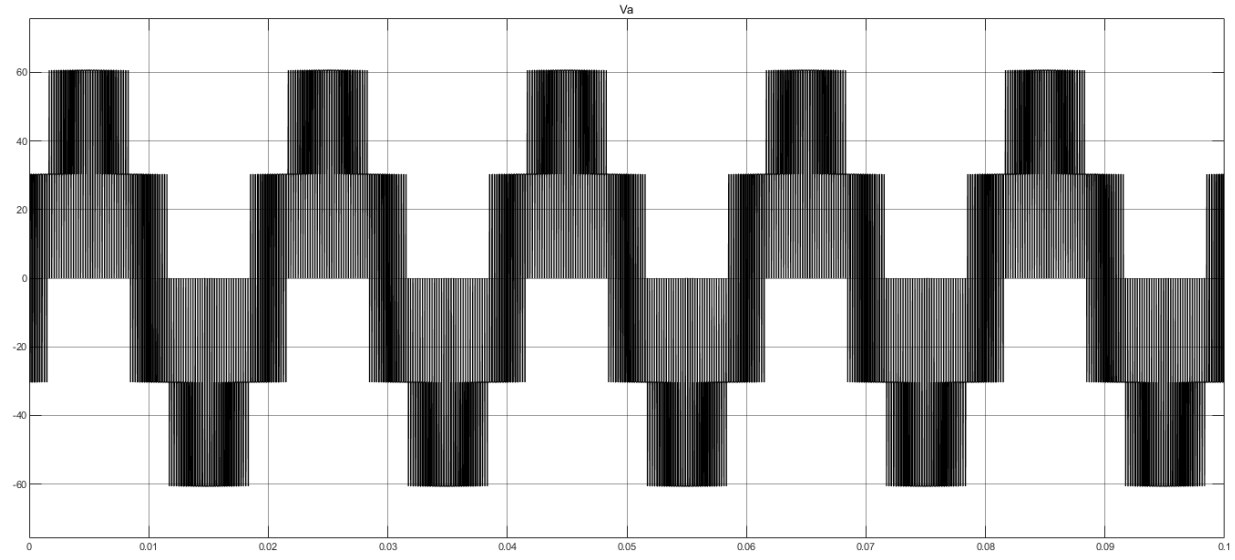

Figure 30 Phase Voltage Output (Va)

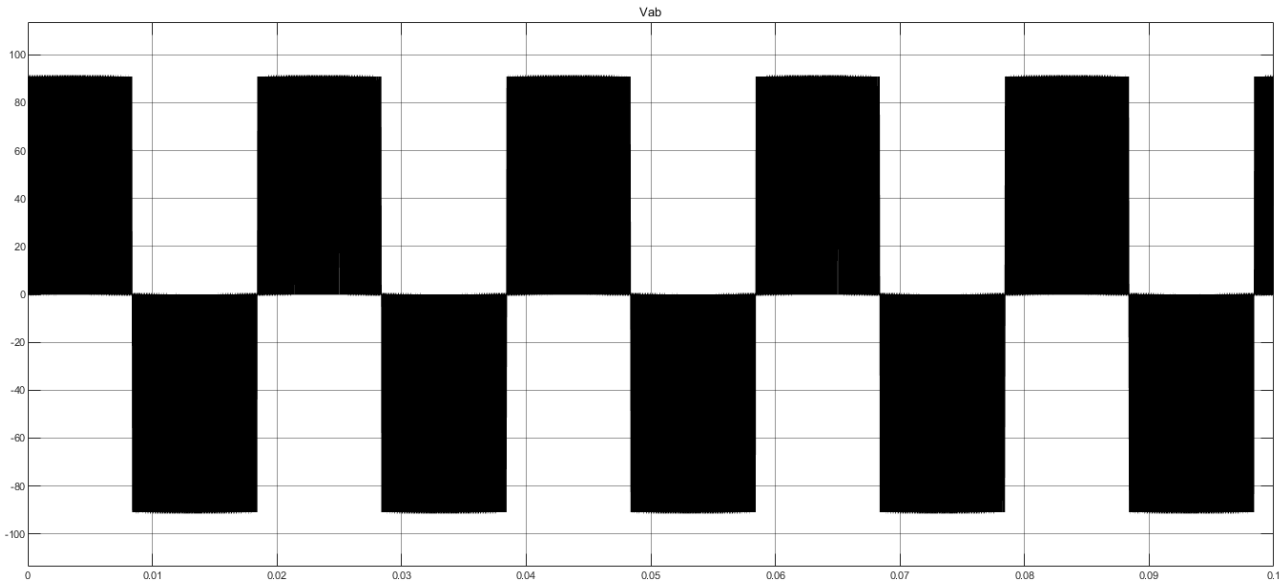

Figure 31 Line Voltage Output (Vab)

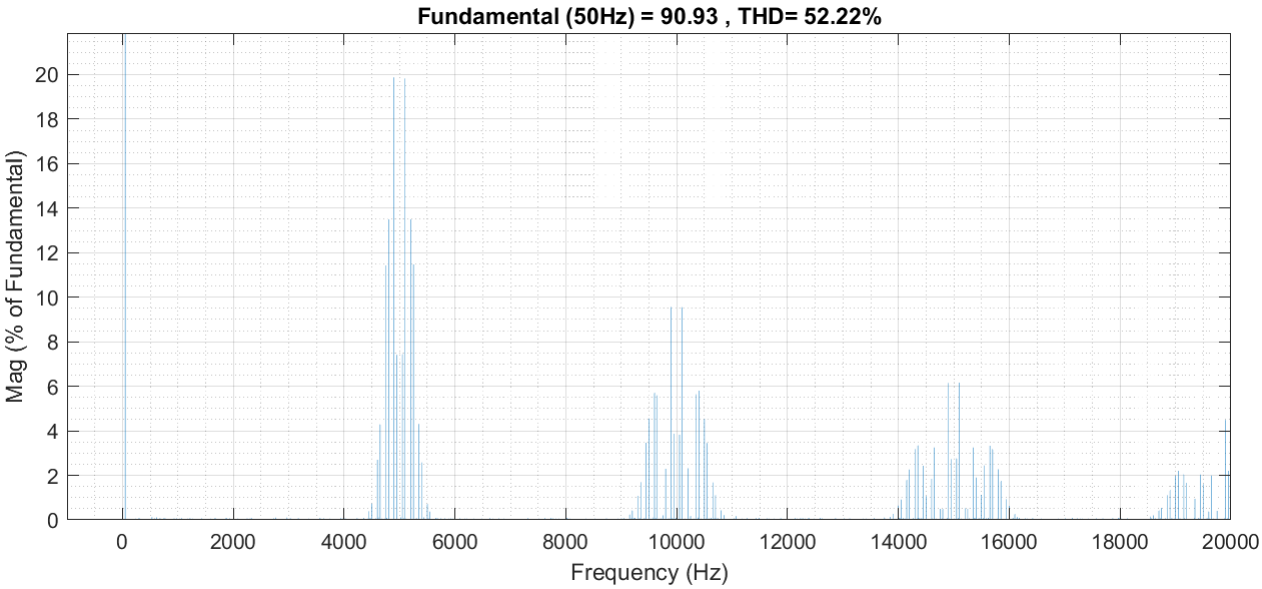

Figure 32 Va Harmonic Spectrum

In comparison with SPWM, this technique boosted the voltage from 78.71 V to 90.93 V. This is an increase of 15.52% in voltage. This exact value of increase was expected based on the impact of 3rd harmonic injection. Also, the THD decreased significantly,

4.1.1.3.3 Space Vector Modulation

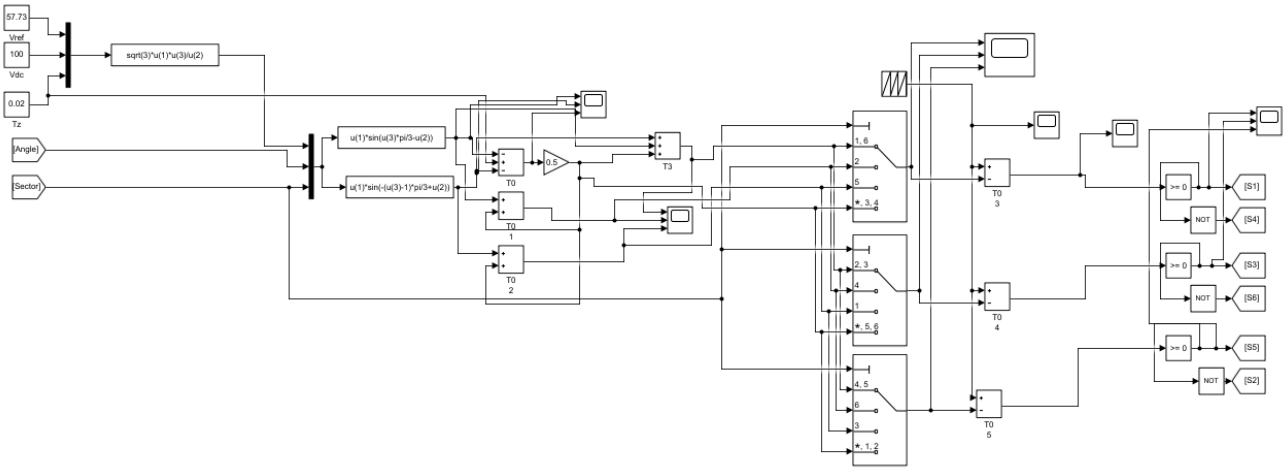

Figure 33 Control Circuit

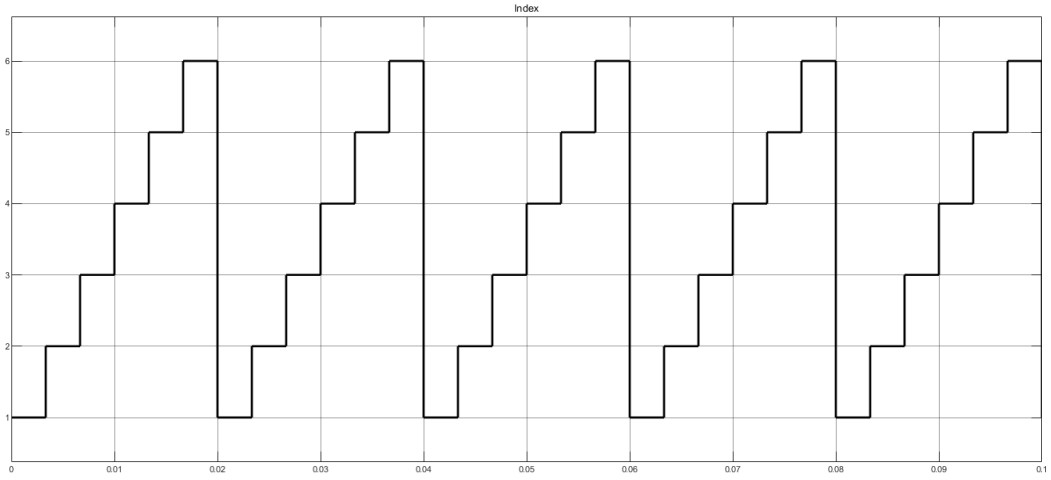

Figure 34 The 6 Sectors

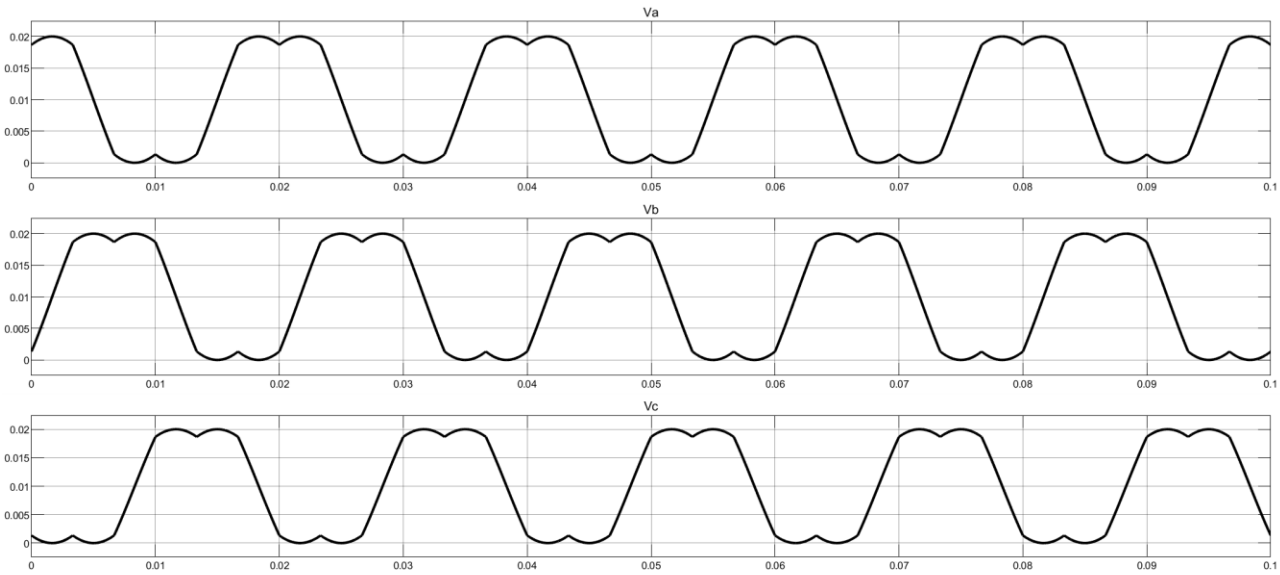

Figure 35 Modulation Signals

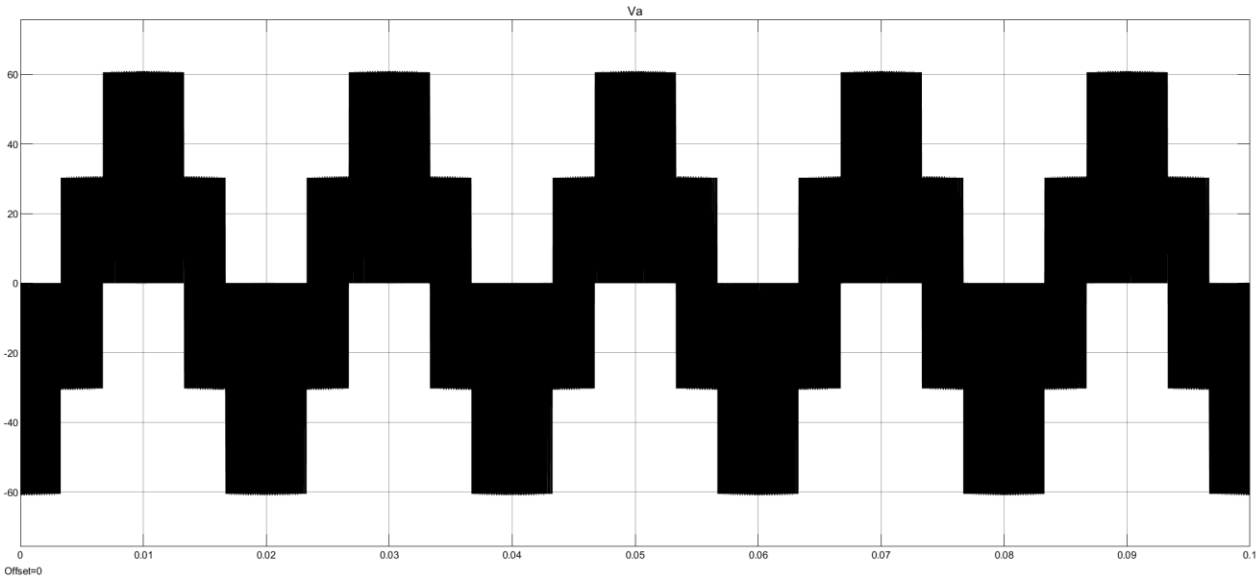

Figure 36 Phase Voltage Output (Va)

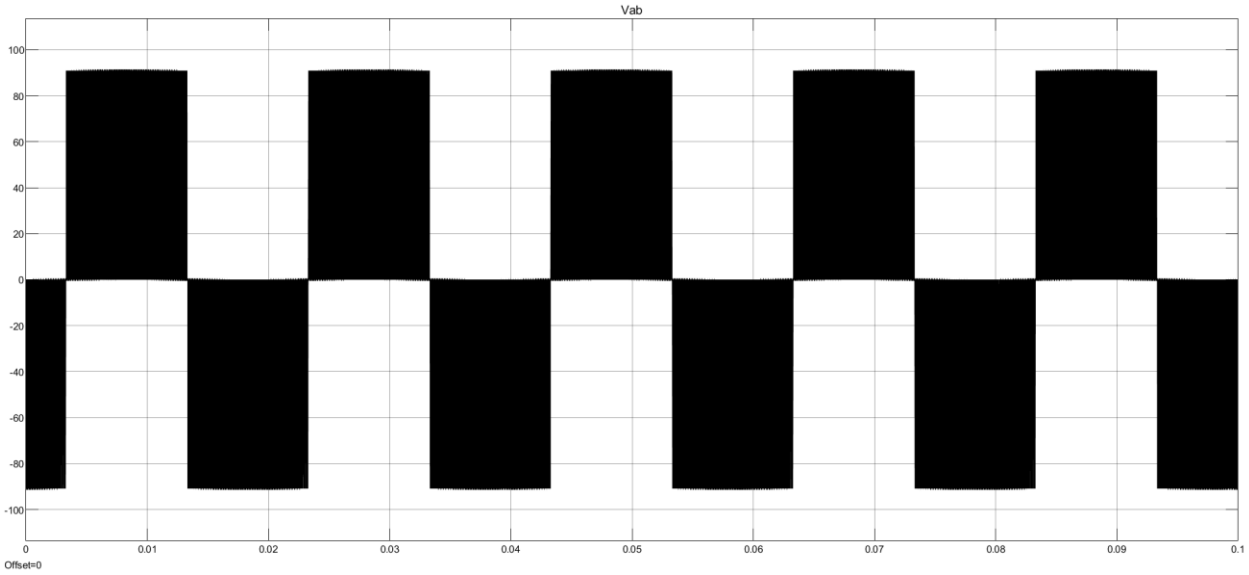

Figure 37 Line Voltage Output (Vab)

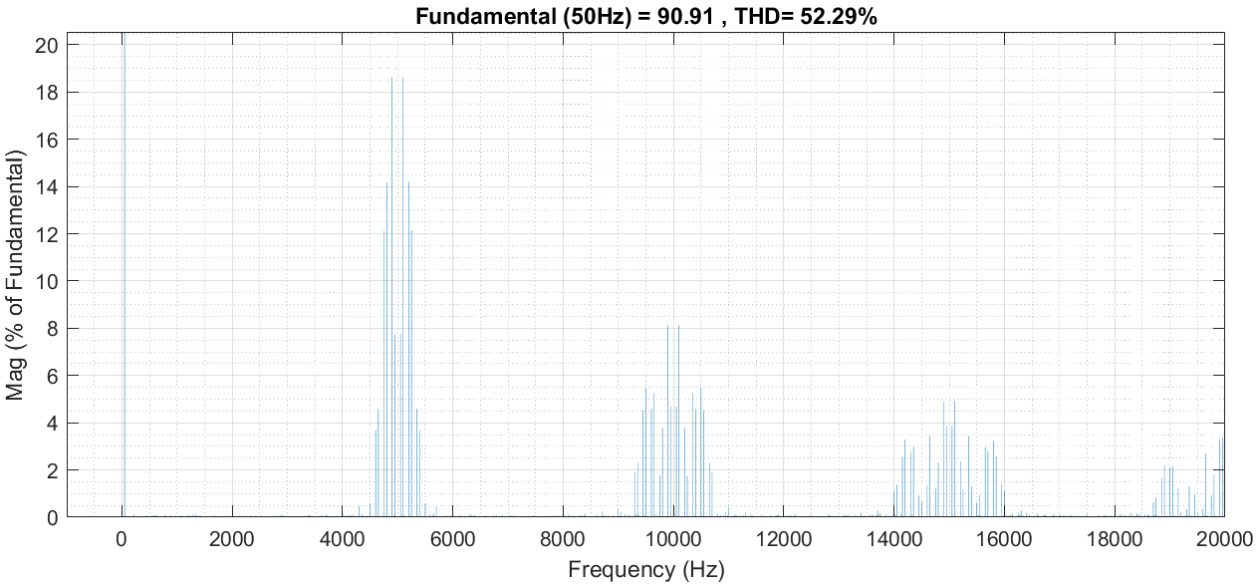

Figure 38 Va Harmonic Spectrum

As expected, the SVM technique came close to the 3rd harmonic injection technique in voltage and harmonic outputs. The main advantage of this technique is the least switching losses it has, since only switch changes at a time.

4.1.1.4 Comparison

These simulations provided a decisive proof that the 3rd harmonic injection outperforms the regular SPWM by boosting the voltage by 15% and decreasing the harmonics. Also, it showed that it performs very similar to the Space Vector Modulation, although the latter technique is much complicated to implement. Its main favor is decreasing the switching losses, since it changes one switch at a time.

Those results were expected. As the theory shows below, the SVM techniques boasts the range of output voltage by a considerable margin in comparison to SPWM.

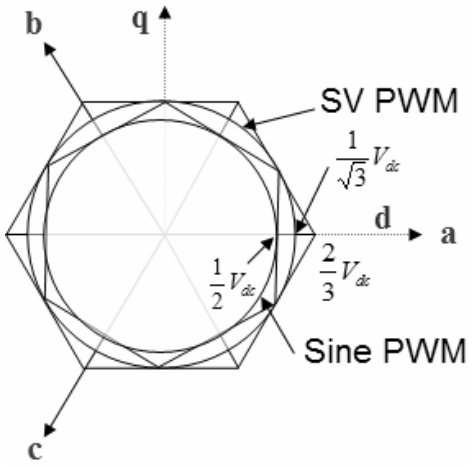

Figure 39 Locus of Modulation Signals Output Voltages [13]

4.1.2 Dual Inverter Drive

4.1.2.1 Schematics

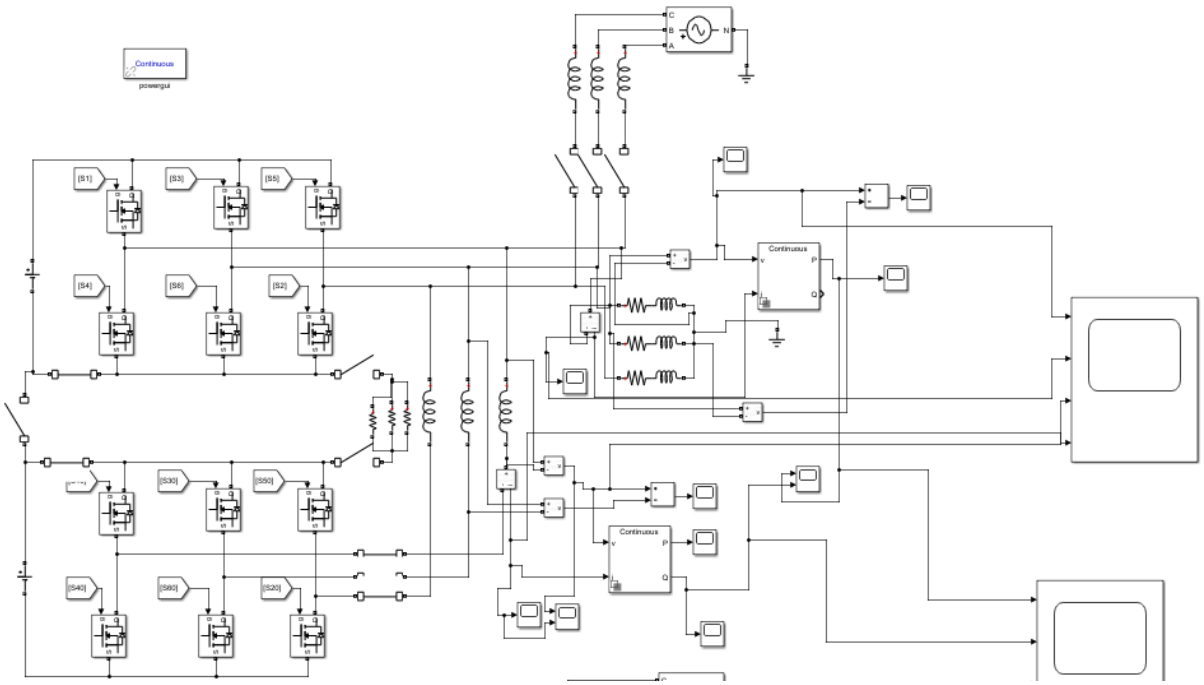

Figure 40 Dual Inverter Drive Simulink Model

4.1.2.2 Parameters

- V_{dc}: 100 V
- Motor Resistance: 0.1 Ω
- Motor Inductance: 471*10-6 H
- Joint Load Inductance: 471*10-6 H
- Grid Voltage: 1000 V
- Carrier Frequency: 5000 Hz
- Modulating Waveform Frequency: 50 Hz

- Modulating Waveform Amplitude: 1
- Third Harmonic Amplitude: 1/6
- Third Harmonic Frequency: 150 Hz

4.1.2.3 Techniques

In this section, the 3rd harmonic injected PWM will be tested on the dual inverter drive. This choice was made based on the superior performance it had on the single inverter model.

4.1.2.3.1 Sinusoidal Pulse Width Modulation

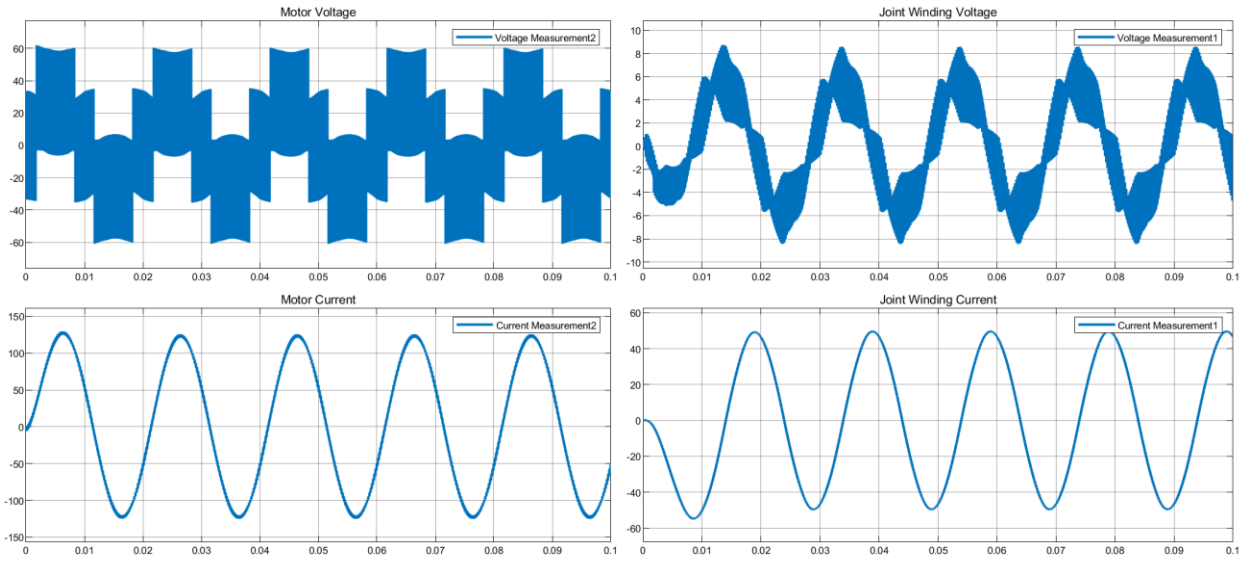

Figure 41 Motor and Joint Winding Voltages and Currents of SPWM

Table 7 Phase Output Voltages and Harmonics of SPWM

	Fundamental Phase Voltage	THD	3rd Harmonic Value
Motor Winding	47.7 V	59.1 %	0.5 %
Joint Load Winding	8.4 V	14.5 %	0.6 %

4.1.2.3.2 Third Harmonic Sinusoidal Pulse Width Modulation

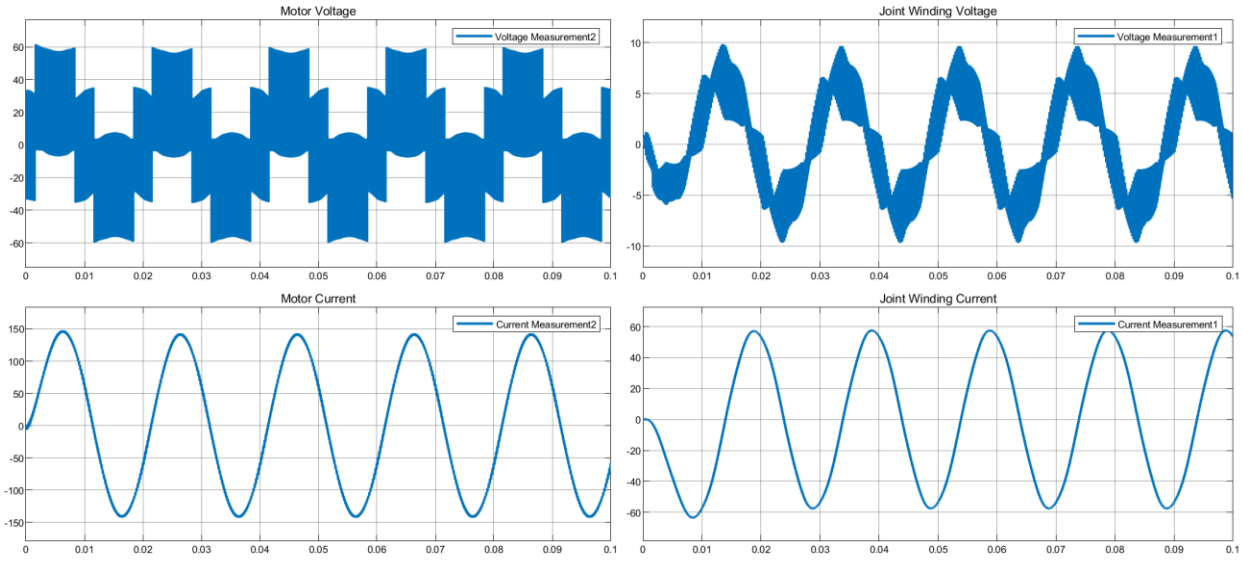

Figure 42 Motor and Joint Winding Voltages and Currents of THISPWM

Table 8 Phase Output Voltages and Harmonics of THISPWM

	Fundamental Phase Voltage	THD	3rd Harmonic Value
Motor Winding	47.1 V	62.4 %	0.3 %
Joint Load Winding	8.4 V	13.2 %	0.4 %

4.1.2.3.3 Space Vector Modulation

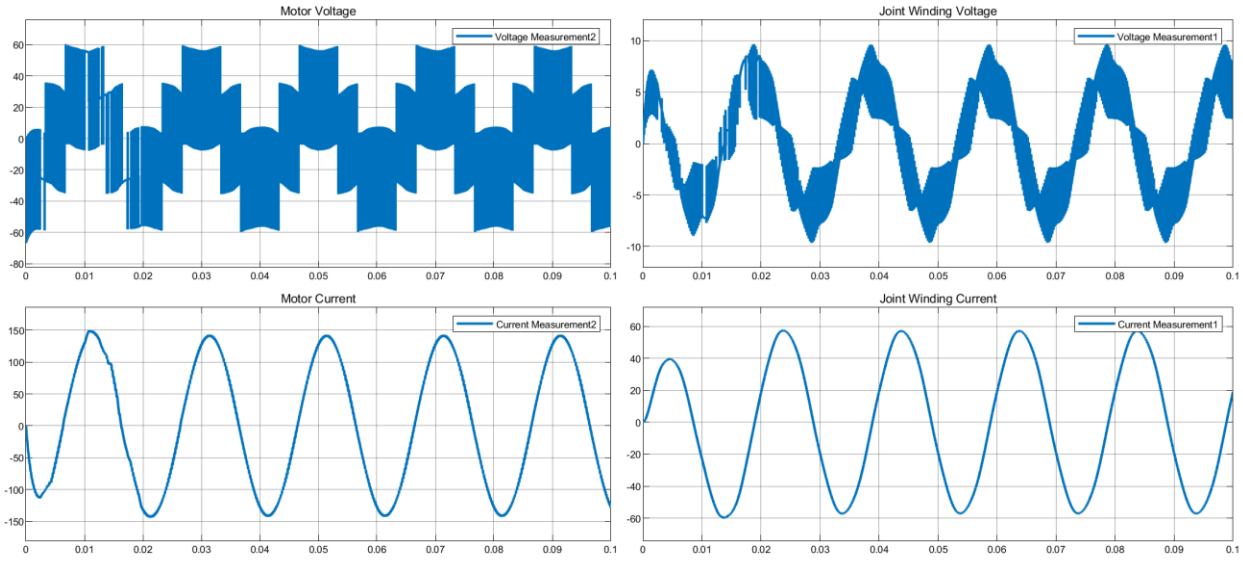

Figure 43 Motor and Joint Winding Voltages and Currents of SVM

Table 9 Phase Output Voltages and Harmonics of SVM

	Fundamental Phase Voltage	THD	3rd Harmonic Value
Motor Winding	47.2 V	61.9 %	0.04 %
Joint Load Winding	8.4 V	15.1 %	0.05 %

4.1.2.3.4 Comparison of Modulation Techniques Performance on Dual Inverters

For phase angle of zero degree between the 2 inverters in SPWM and THISPWM, the values of fundamental phase voltages and total harmonic distortion came close in the 3 techniques. The major difference was the low 3rd harmonic value in SVM compared to the other techniques where it was 1/10 or less of that. However, the major defect of this technique is the complexity of the control circuit. That makes power flow distribution harder to implement in SVM than in the other techniques.

4.1.2.4 Phase Effect

The previous section showed that the voltage levels at the different loads is uneven. In this section, the phase angle between the gates of the 2 inverters will be changed from 0 to 180 in 30-degree increments. Recorded voltages, harmonics and powers of loads will be compared.

4.1.2.4.1 0 Degrees

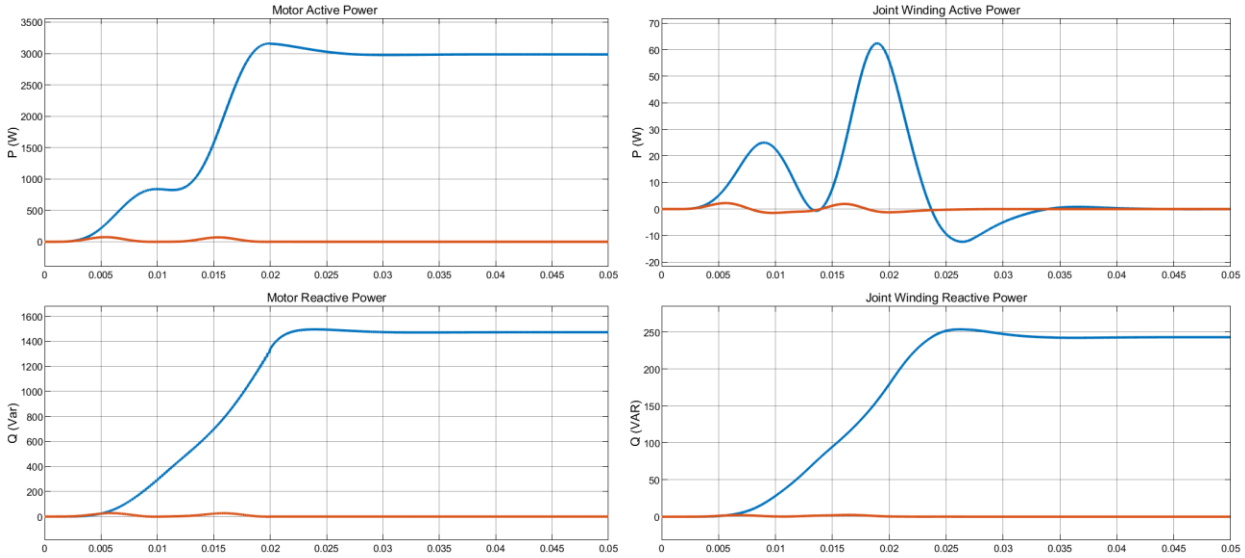

Figure 44 Active and Reactive Power Phase Measurements at 0 Degrees

Table 10 Output Readings at 0 Degrees Phase Angle

	Va (fundamental)	Va THD	Active Power	Reactive Power	Apparent Power
Motor	47.1	62.2	2985	1472	3328
Joint Winding	8.5	13.9	0	243	243

4.1.2.4.2 30 Degrees

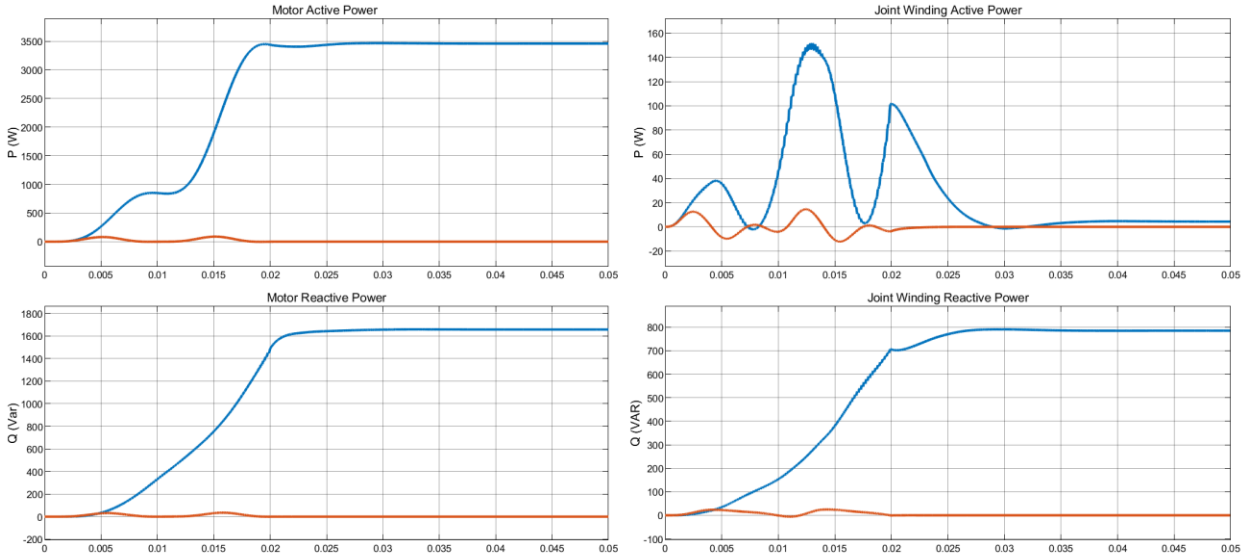

Figure 45 Active and Reactive Power Phase Measurements at 30 Degrees

Table 11 Output Readings at 30 Degrees Phase Angle

	Va (fundamental)	Va THD	Active Power	Reactive Power	Apparent Power
Motor	50.5	53.8	3459	1656	3834
Joint Winding	15.2	258.1	4	784	784

4.1.2.4.3 60 Degrees

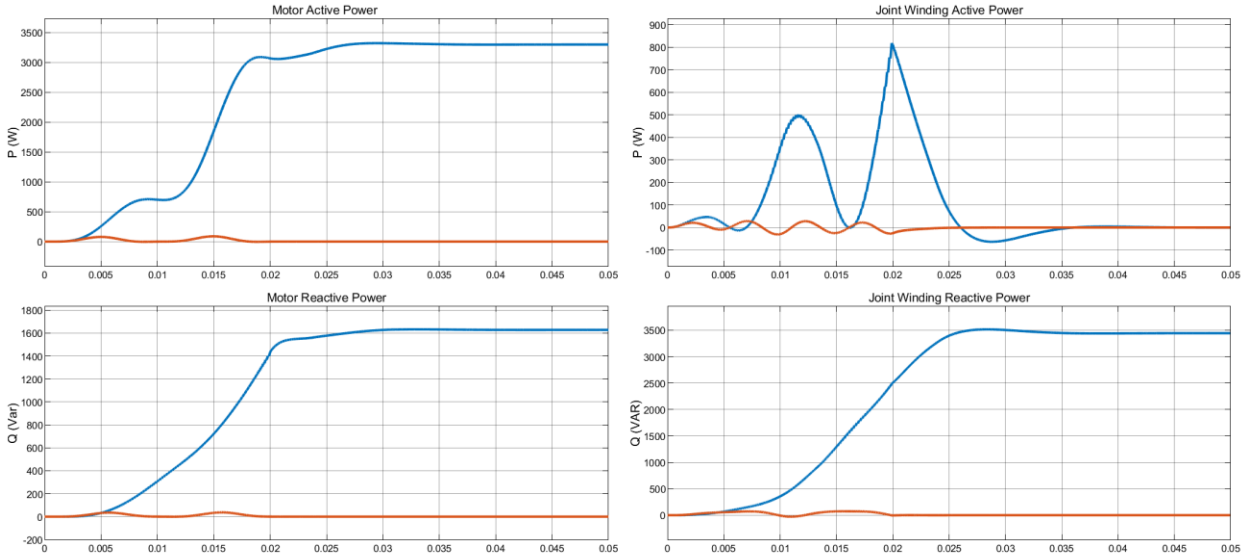

Figure 46 Active and Reactive Power Phase Measurements at 60 Degrees

Table 12 Output Readings at 60 Degrees Phase Angle

	Va (fundamental)	Va THD	Active Power	Reactive Power	Apparent Power
Motor	49.6	49.1	3301	1628	3680
Joint Winding	31.9	139.1	0	3443	3443

4.1.2.4.4 90 Degrees

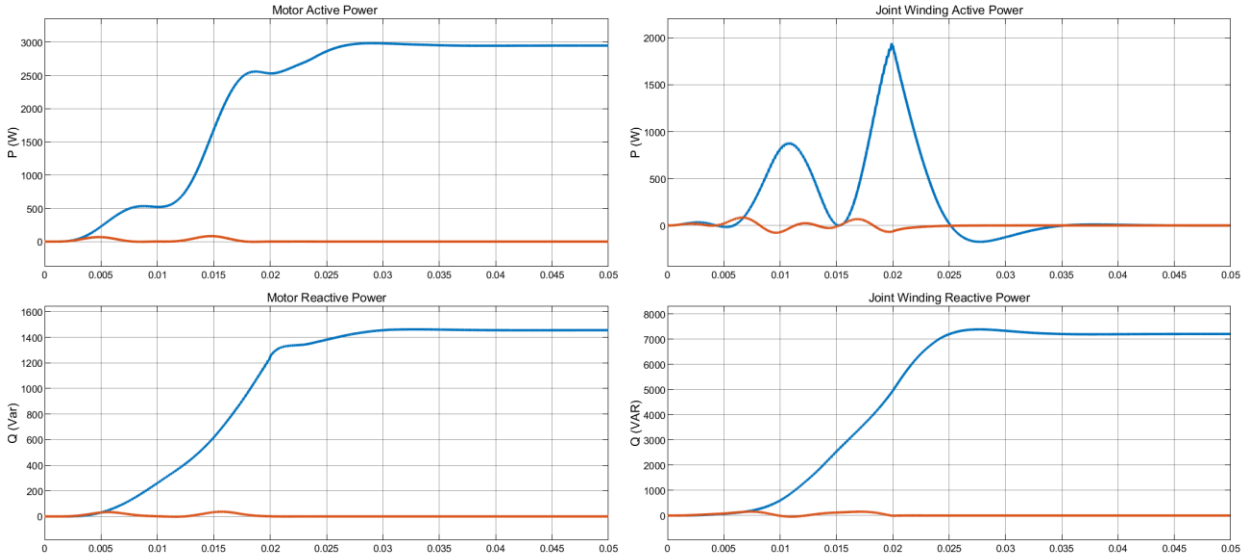

Figure 47 Active and Reactive Power Phase Measurements at 90 Degrees

Table 13 Output Readings at 90 Degrees Phase Angle

	Va (fundamental)	Va THD	Active Power	Reactive Power	Apparent Power
Motor	47.0	47.4	2951	1455	3290
Joint Winding	46.3	93.9	-1	7203	7203

4.1.2.4.5 120 Degrees

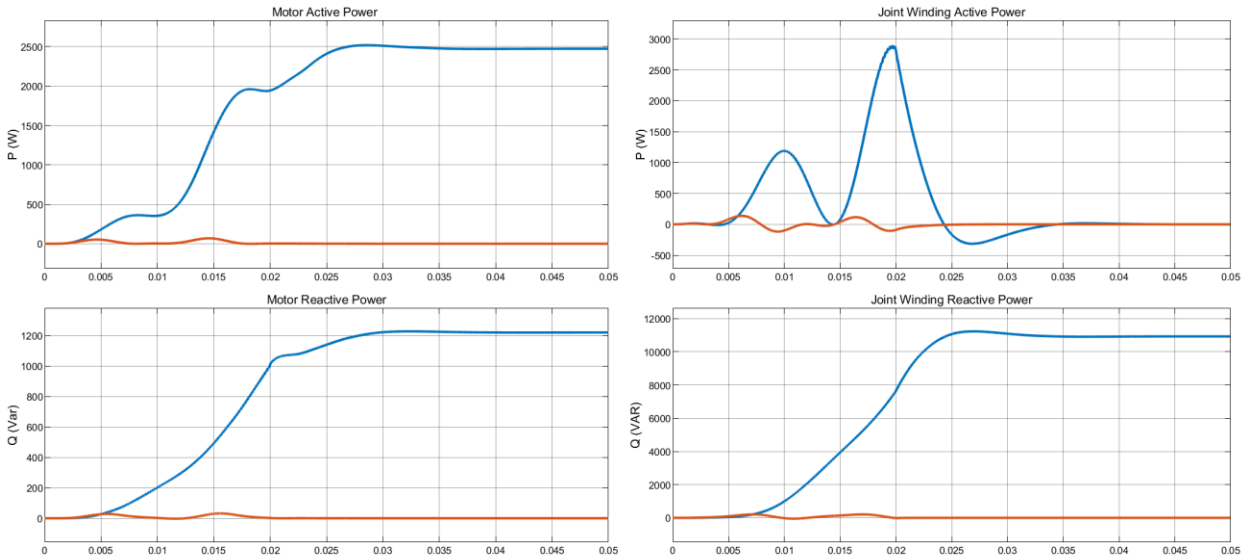

Figure 48 Active and Reactive Power Phase Measurements at 120 Degrees

Table 14 Output Readings at 120 Degrees Phase Angle

	Va (fundamental)	Va THD	Active Power	Reactive Power	Apparent Power
Motor	43.0	48.8	2473	1220	2757
Joint Winding	57.1	71.5	0	10921	10921

4.1.2.4.6 150 Degrees

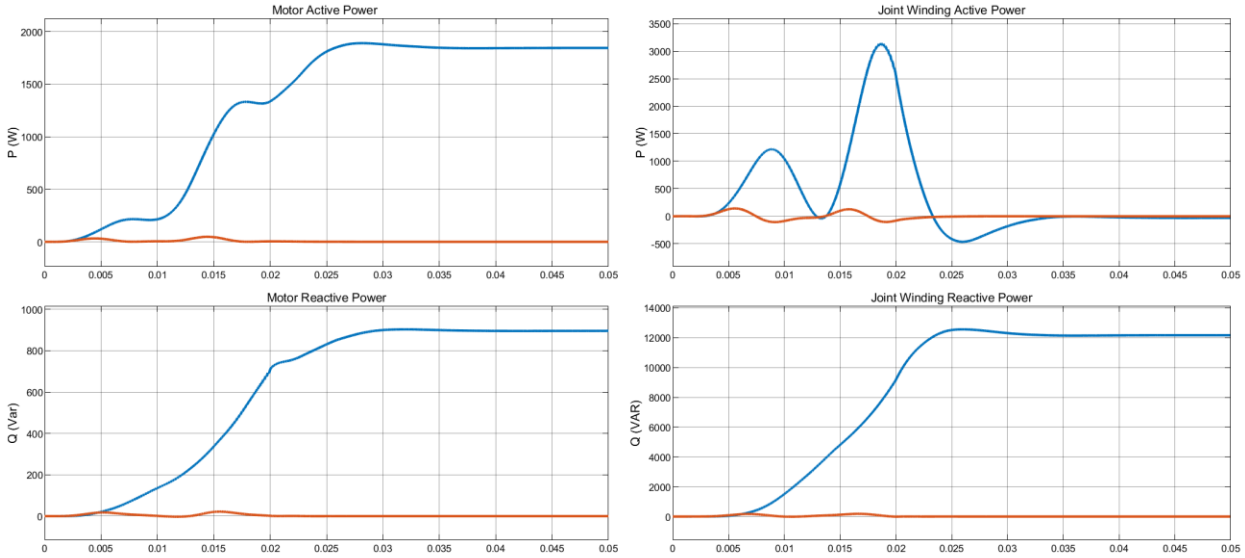

Figure 49 Active and Reactive Power Phase Measurements at 150 Degrees

Table 15 Output Readings at 150 Degrees Phase Angle

	Va (fundamental)	Va THD	Active Power	Reactive Power	Apparent Power
Motor	36.8	58.8	1844	896	2050
Joint Winding	59.9	50.4	-29	12162	12162

4.1.2.4.7 180 Degrees

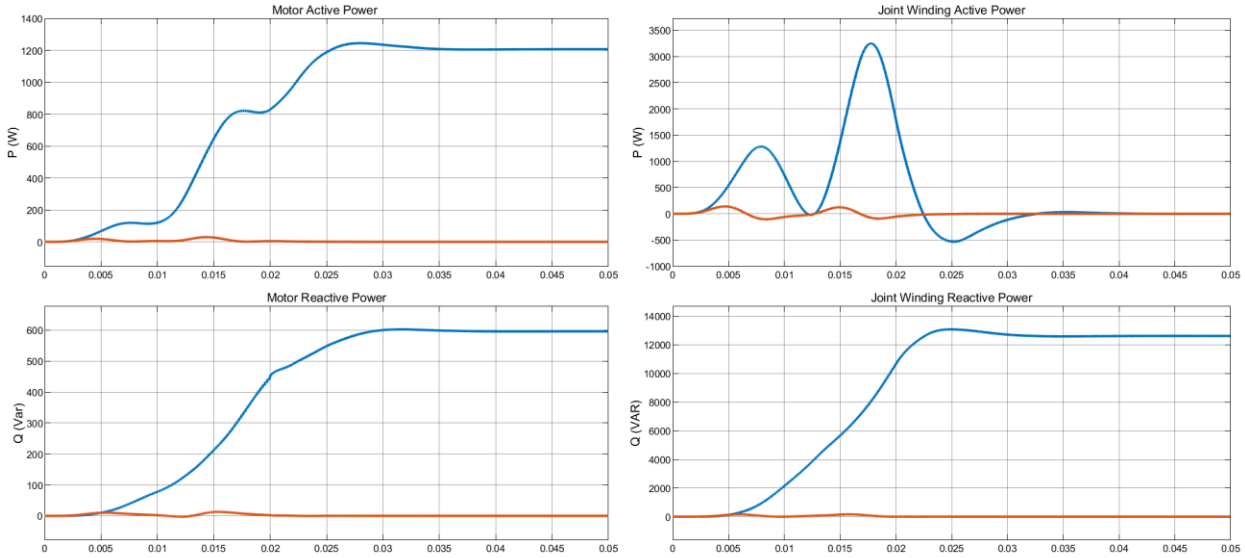

Figure 50 Active and Reactive Power Phase Measurements at 180 Degrees

Table 16 Output Readings at 180 Degrees Phase Angle

	Va (fundamental)	Va THD	Active Power	Reactive Power	Apparent Power
Motor	30.1	76.6	1208	595	1346
Joint Winding	61.4	43.7	0	12612	12612

4.1.2.4.8 Comparison

4.1.2.4.8.1 Voltage and Harmonics Variations

This table summarizes the outputs from all angle variation trials.

Table 17 All Phase Angle Variations Comparison

Angle	Motor Fundamental Phase Voltage	Joint Winding Fundamental Phase Voltage	Motor Phase Voltage THD	Joint Winding Phase Voltage THD	Motor Active Power by Phase	Motor Reactive Power by Phase	Joint Winding Active Power by Phase	Joint Winding Reactive Power by Phase
0	47.1	8.5	62.2	13.9	2985	1472	0	243
30	50.5	15.2	53.8	258.1	3459	1656	4	784
60	49.6	31.9	49.1	139.1	3301	1628	0	3443
90	47.0	46.3	47.4	93.9	2951	1455	-1	7203
120	43.0	57.1	48.8	71.5	2473	1220	0	10921
150	36.8	59.9	58.8	50.4	1844	896	-29	12162
180	30.1	61.4	76.6	43.7	1208	595	0	12612

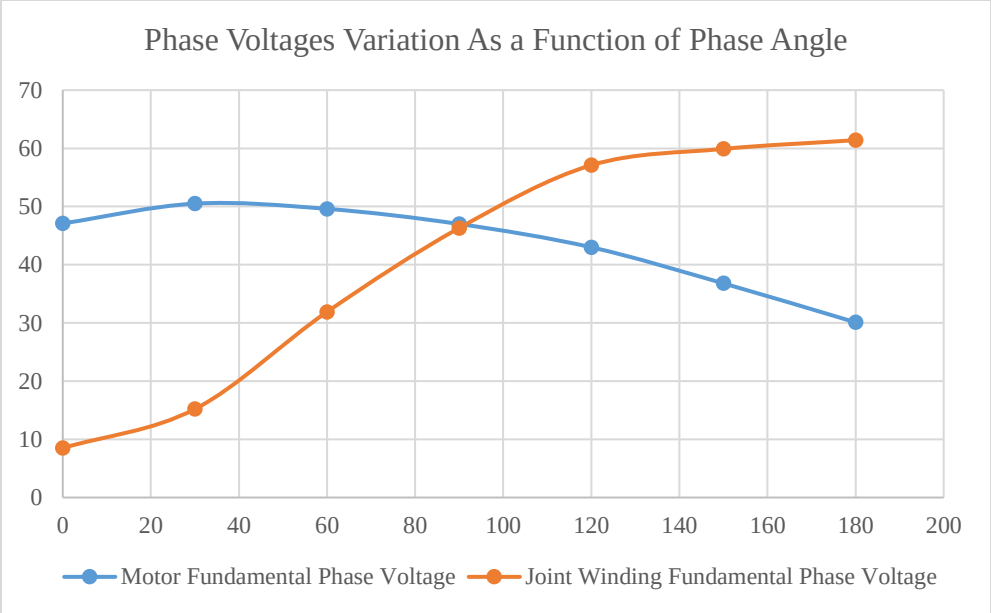

Figure 51 Phase Voltages Variation As a Function of Phase Angle

As it can be clearly seen from the graph above, as the angle increases from 0° to 180°, the motor phase voltage decreases while the joint winding phase voltage increases. The two voltages would be equal 46 V around 90°. This means that changing phase angle wisely can achieve desired equal voltages even if the loads are different.

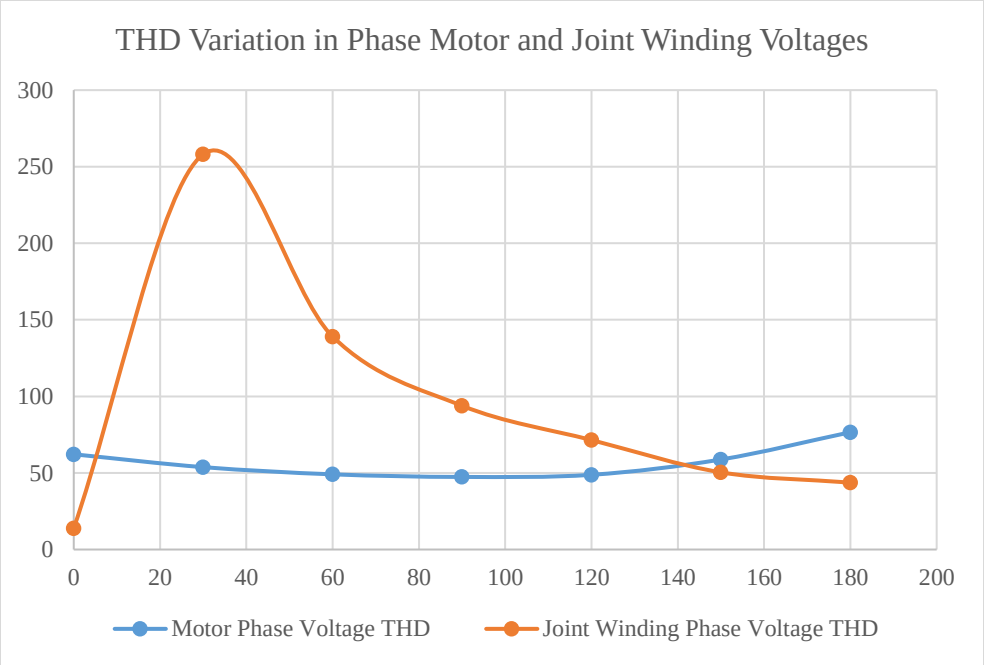

Figure 52 THD Variation in Phase Motor and Joint Winding Voltages

The figure above shows the variation of THD with phase angle change. With the exception of angle 0, the THD of the motor voltage slightly increases while the angle increases to reach 180°, while the THD of joint winding voltage decreases significantly. The THD of both voltages would be close to 50% around 140° phase difference. This level of distortion would be acceptable in comparison with other settings with it soars much higher than that as for the case of 30°. It worths noting that overall distortion can be improved by using filters, but at this level, the main concern is to analyze the voltage performance with angle variation independent of other factors like filters.

4.1.2.4.8.2 Power Variations

Table 18 Single Phase and Three Phase Apparent Power Calculations

	Motor Apparent Power by Phase	Motor Apparent Power of Three Phases	Joint Winding Apparent Power by Phase	Joint Winding Apparent Power of Three Phase	Total Loads Apparent Power	Total Loads Active Power	Total Loads Reactive Power	Ratio of Active Power to Apparent Power Totals	Ratio of Reactive Power to Apparent Power Totals
0	3328	9985	243	729	10714	8955	5145	0.836	0.480
30	3835	11505	784	2352	13857	10389	7320	0.750	0.528
60	3681	11042	3443	10329	21371	9903	15213	0.463	0.712
90	3290	9871	7203	21609	31480	8850	25974	0.281	0.825
120	2758	8273	10921	32763	41036	7419	36423	0.181	0.888
150	2050	6150	12162	36486	42637	5445	39174	0.128	0.919
180	1347	4040	12612	37836	41876	3624	39621	0.087	0.946

The table above shows the apparent power ($S = \sqrt{P^2 + Q^2}$) per phase, and per three phases by multiplying by three for motor and joint load. Also, it includes the total active, reactive and apparent powers for total circuit loads, and the ratio of total active and reactive powers to the total apparent power.

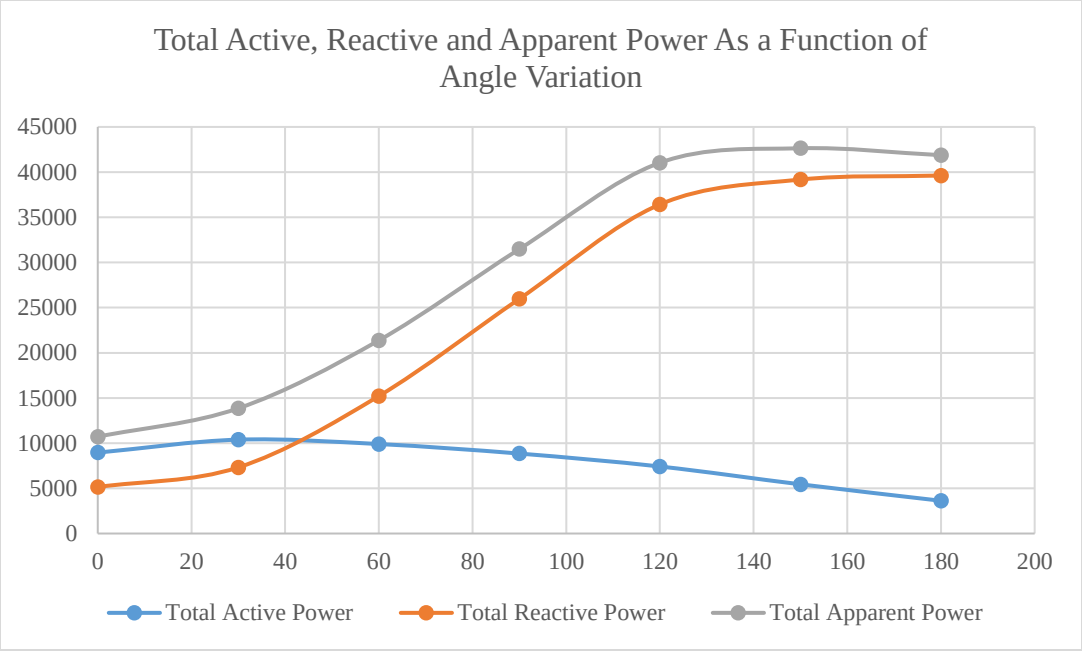

Figure 53 Total Active, Reactive and Apparent Power As a Function of Angle Variation

The figure shows clearly that as the phase angle increases from 0° to 180°, the total active power decreases slightly but the surge of reactive power boasts the overall apparent power until it forms a plateau when the angle surpasses 120°. This signifies close relation between phase angle and active and reactive power distribution. For an angle around 45°, the active and reactive powers can be equal around 10000 W and Var respectively.

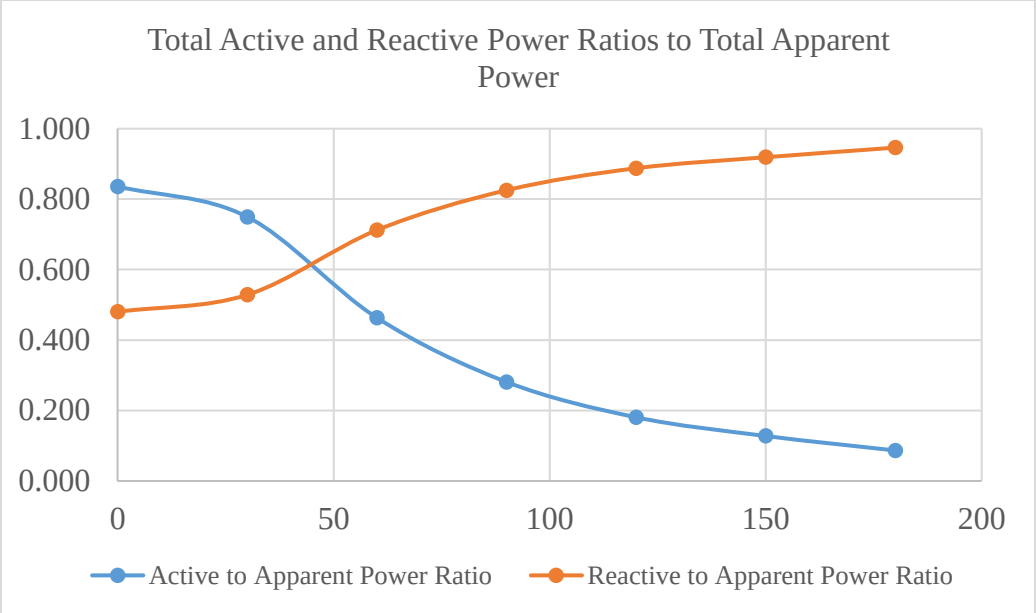

Figure 54 Total Active, Reactive and Apparent Ratios to Total Apparent Power

The figure above shows that the ratio of reactive power to apparent power rises from 50% to 90% as the angle varies from 0° to 180°. In the same interval, the ratio of active power decreases massively from 80% to almost 10%. Around 45°, the two ratios equalize around 60%.

The table below introduces ς, which is the tan inverse of the reactive power to active power (Q/P). Then, as an assumption, the cosine of this obtained angle is multiplied by the measured apparent power S to obtain a calculated value of power called P_{cal}. Similarly, Q_{cal} will be obtained. Then, the errors between these calculated powers and the already measured powers from the model will be obtained.

Table 19 Active and Reactive Power Errors Calculation

Angle	Ratio of Active Power to Apparent Power Totals (P/S)	Ratio of Reactive Power to Apparent Power Totals (Q/S)	Ratio of Reactive Power to Active Power Totals (Q/P)	$\tan^{-1}(Q/P) = \varsigma$	$P_{cal=} S * \cos(\varsigma)$	$Qcal=S * \sin(\varsigma)$	$Perror=(P_{cal}-P)/P$ %	$Qerror=(Q_{cal}-Q)/Q$ %
0	0.836	0.480	0.575	29.879	9290	5337	3.74	3.74
30	0.750	0.528	0.705	35.168	11328	7981	9.03	9.03
60	0.463	0.712	1.536	56.938	11659	17910	17.73	17.73
90	0.281	0.825	2.935	71.185	10153	29797	14.72	14.72
120	0.181	0.888	4.909	78.487	8190	40210	10.40	10.40
150	0.128	0.919	7.194	82.087	5870	42231	7.80	7.80
180	0.087	0.946	10.933	84.774	3814	41702	5.25	5.25

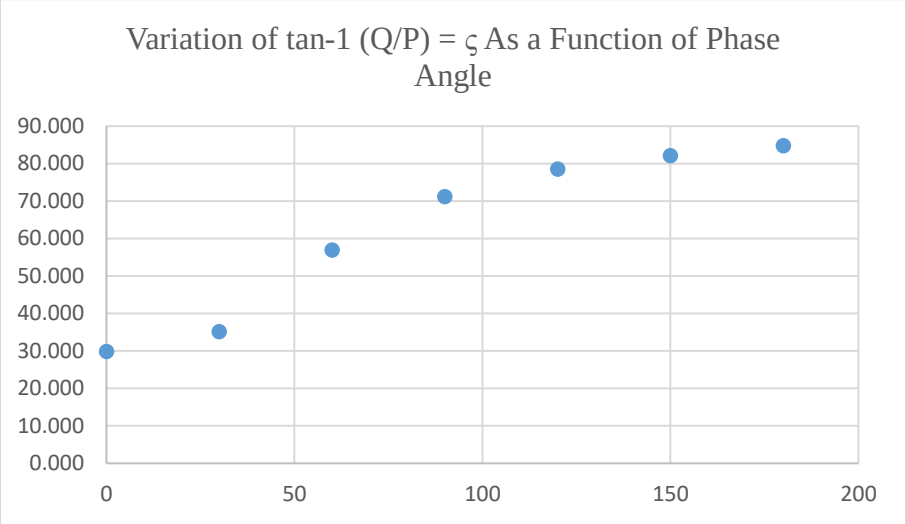

Figure 55 Variation of ς As a Function of Phase Angle

The figure above shows the increase of the calculated angle ς from 30° to 85° as the phase angle increases from 0° to 180°. The angle seems reaching a plateau after crossing 120°.

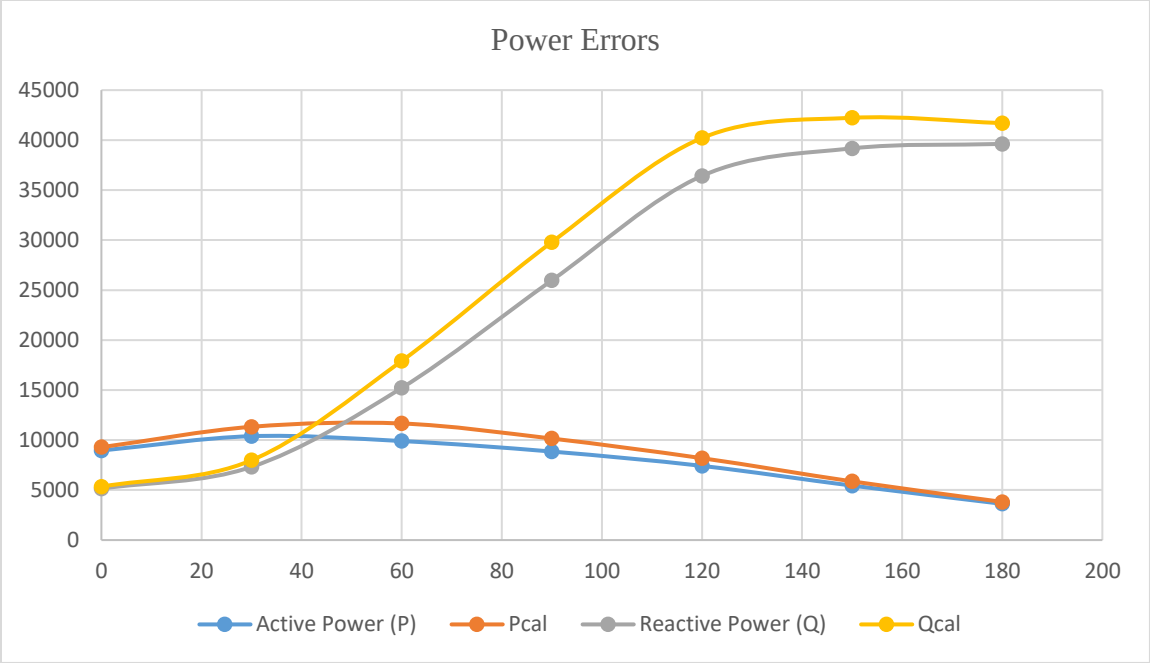

Figure 56 Power Errors Between Measured and Calculated Values

The figure above shows the differences between the measured and calculated active and reactive powers. The difference gets smaller toward 0° or to toward 180°, while it maximizes in the middle around 90°.

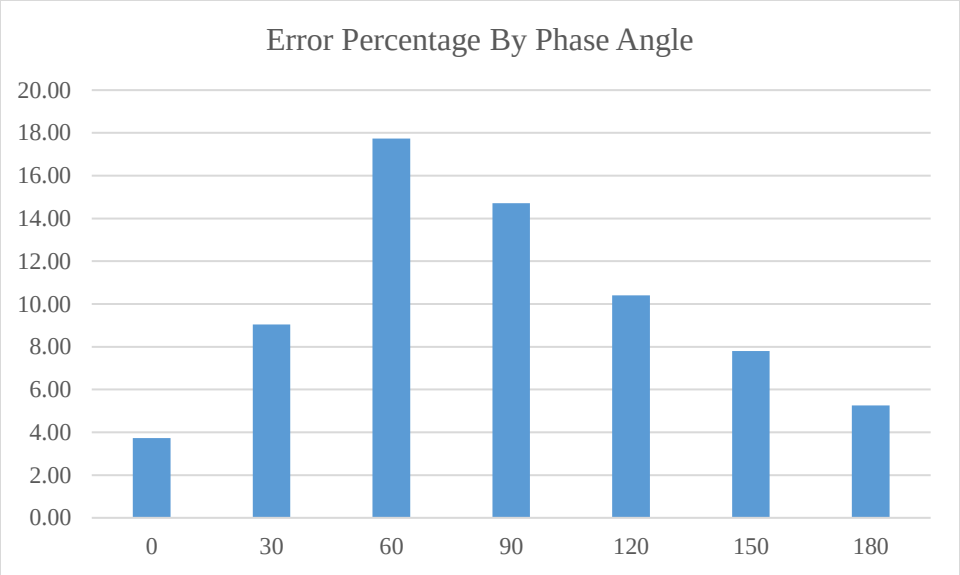

Figure 57 Error Percentage By Phase Angle Variation

This figure shows clearly the errors between measured powers and calculated powers by assumption. The error is minimal at 0° (4%) and then at 180° (5%), while it maximizes on 60° at 18%.

4.1.2.5 Cases

This section will show the voltage and current readings of the loads in different scenarios.

4.1.2.5.1 Single Inverter Operation

In this case, only the upper inverter will operate, closely similar to a single three phase inverter. The grid, resistance bank, joint winding and the lower inverter are all disconnected.

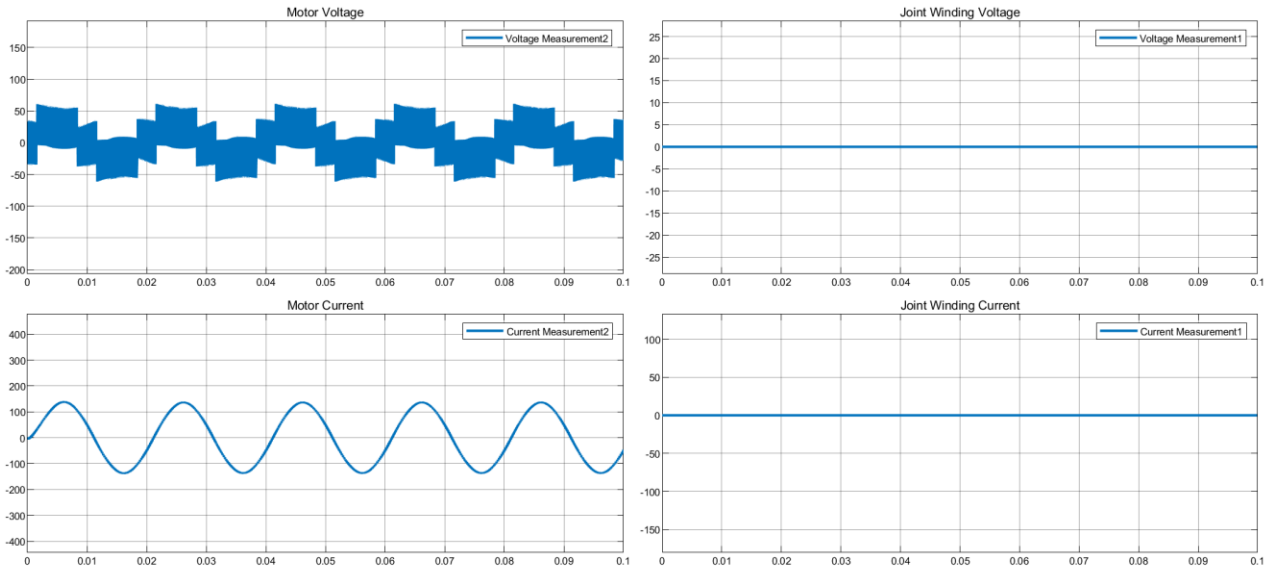

Figure 58 Current and Voltage Outputs of Single Inverter Operation

As expected, only the motor is running.

4.1.2.5.2 Dual Inverter Operation

In this case, both inverters are running. The joint load is connected in additional to the motor. The grid is still disconnected.

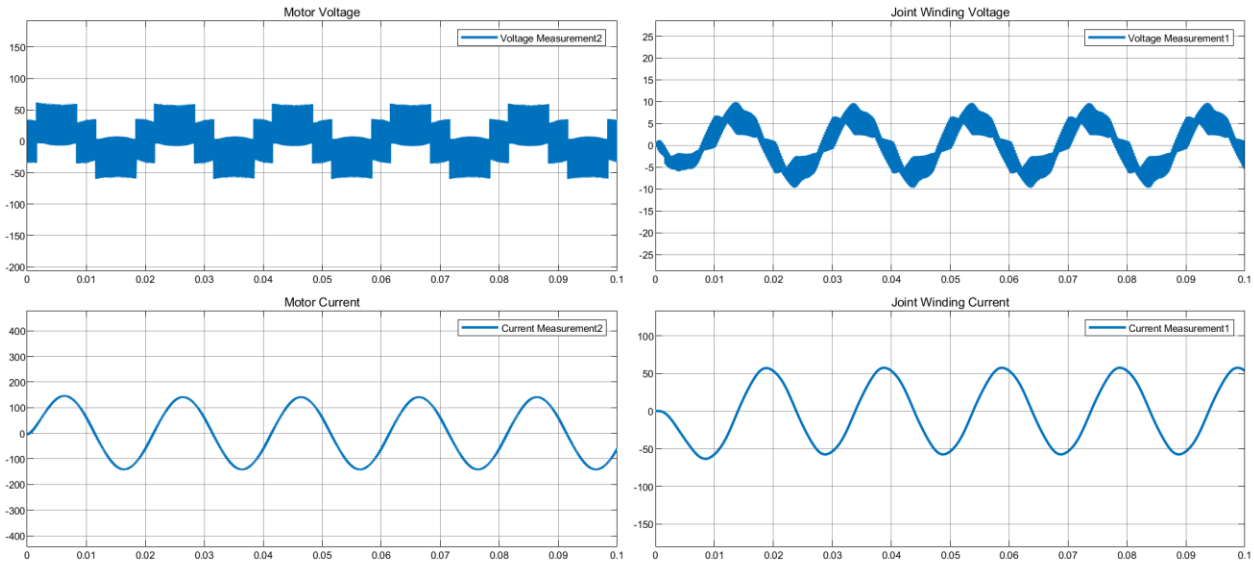

Figure 59 Current and Voltage Outputs of Dula Inverter Operation

Both loads are receiving power, but not in even amounts.

4.1.2.5.3 Dual Inverter Operation with Grid Connection

This case is a typical example when the grid is connected to the drive. Supposedly, the size of the grid will impact the power flow distribution on the system.

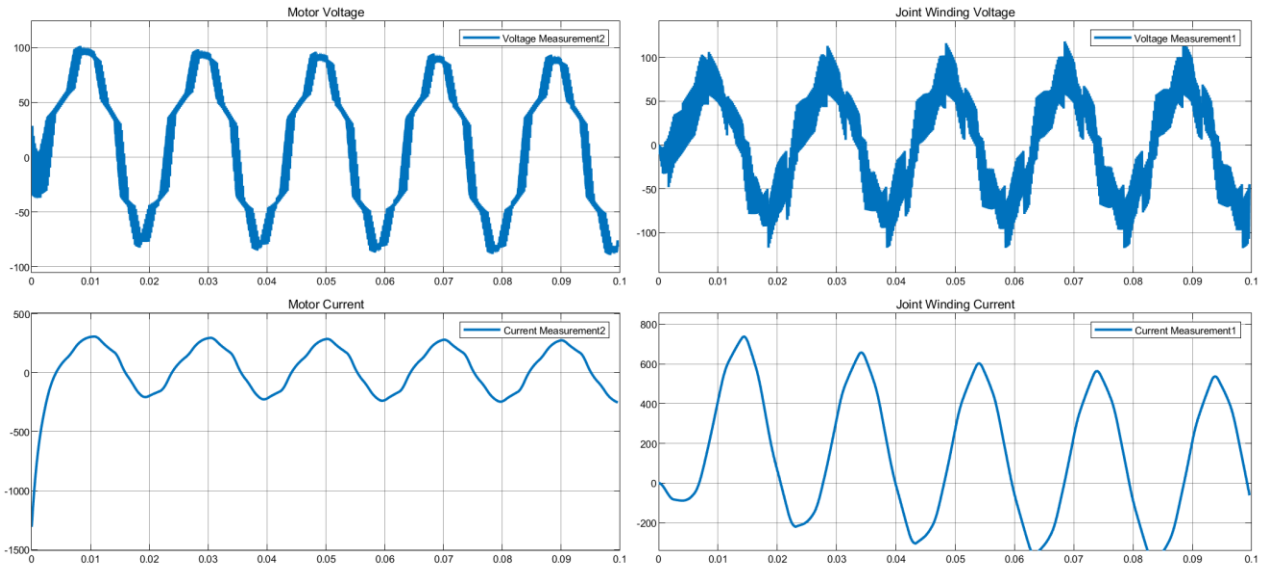

Figure 60 Current and Voltage Outputs of Dual Inverter Operation with Grid

Clearly, the circuit experienced a case similar to a power flow exchange, like charging and discharging to grid. Large current was traversing in the joint winding. But the circuit was able to achieve stability soon. The distortion of the waves is quite high.

4.1.2.5.4 Grid Only Operation

In this case, the inverters are turned off and the grid is connected to the circuit. The motor and joint winding performance will be affected by grid voltage only.

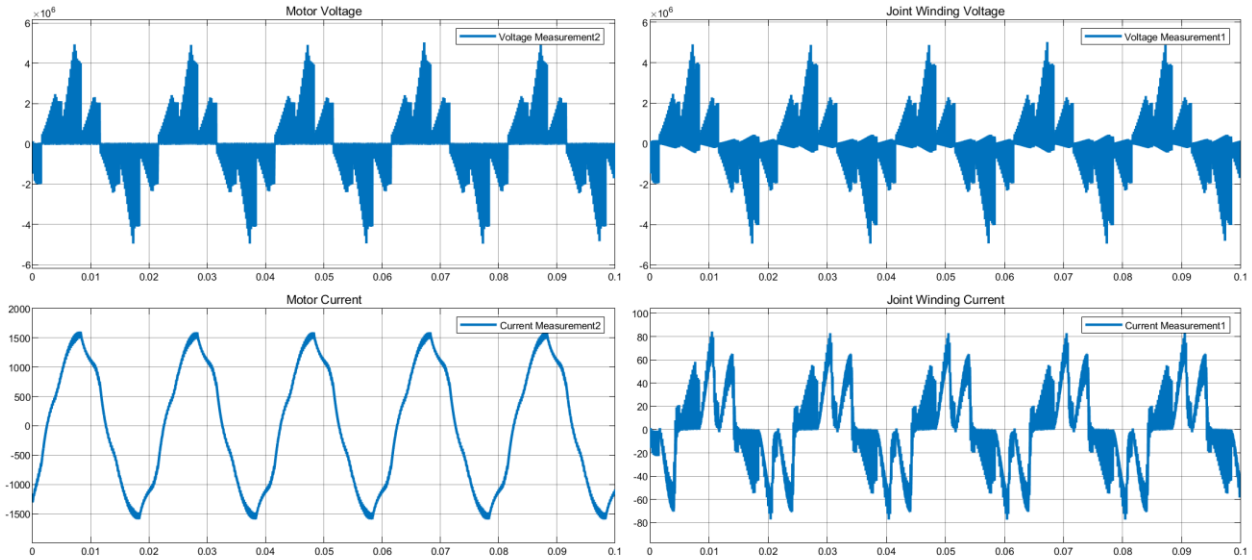

Figure 61 Current and Voltage Outputs of Grid Only Operation

Clearly, since the inverters are absent, the tiny loads compared to the grid experienced a state of fault. The values of current and voltage were stellar, and the circuit components are expected to breakdown. This case should be avoided.

4.1.2.6 Resistance 'Buffer' Effect

This section aims to study the impact of the added resistance bank in faulted operation. The assumption is that the circuit faulted. Resistance will be connected and disconnected to see the difference on active and reactive power readings across the loads.

4.1.2.6.1 Operation without Resistance

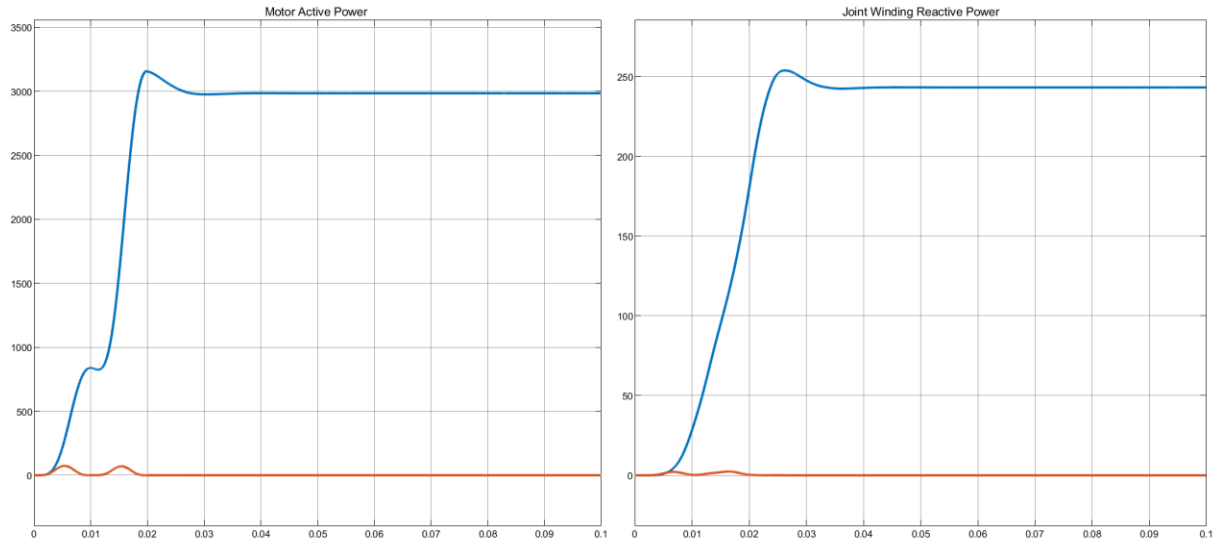

Figure 62 Loads Powers without Resistance Connection

4.1.2.6.2 Operation with Resistance

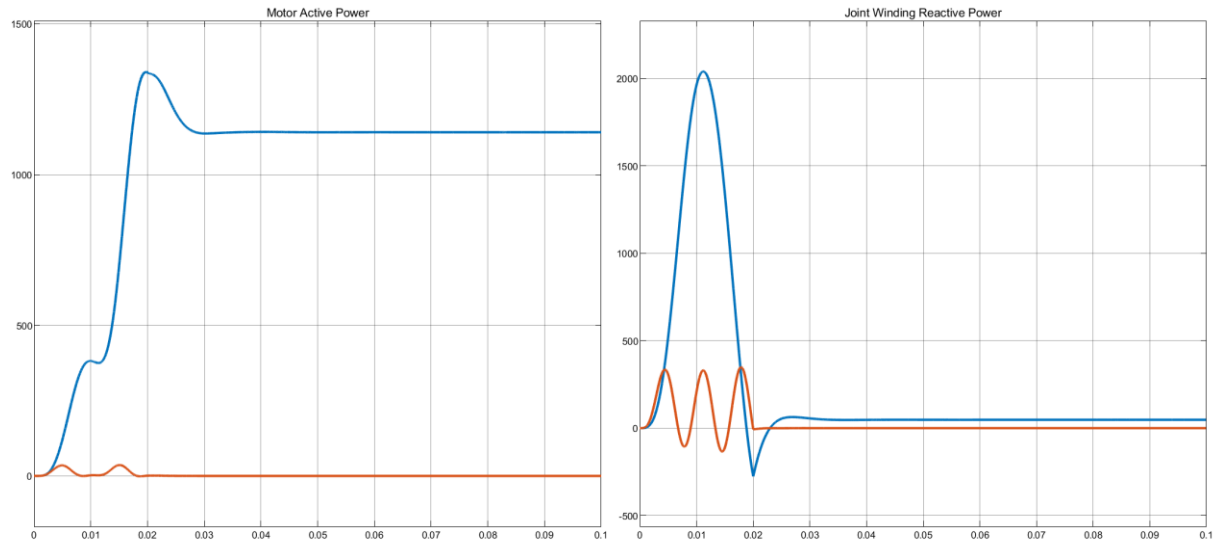

Figure 63 Loads Powers with Resistance Connection

The loads active and reactive powers came significantly less with the addition of the resistance bank. This is expected, since the resistance will modify the impedance by adding an additional path for the current to circulate. Thus, the power at the loads will decrease, and that means less voltage and current ratings.

4.1.2.7 Leakage Current

The leakage current in a three-phase inverter strictly correlates with the common mode voltages. The common mode voltage is the voltage difference between the power source and the neutral point of the three-phase load. Then, the leakage current through circuit grounds will be limited by minimizing the common mode voltages where V_{cm} is equal to $\frac{Van+Vbn+Vcn}{3}$. The common mode leakage current can be derived from V_{cm} by applying the derivative of current with time. Then, I_{cm} is equal to $C* \frac{dVcm}{dt}$. In this section, the leakage currents through grounds will be measured in the same circuit while applying the different modulation techniques. The purpose is to study the effect of modulation techniques on the leakage currents while applying same circuit conditions.

4.1.2.7.1 Leakage Current in THISPWM Case

As the figures below show, a small leakage current to the order of 10^{-6} A is present when the grid is connected while dual inverter drive operation. In the second case, when the grid is disconnected, a very small leakage current to the order of 10^{-14} A still exist at the load grounding. However, it's negligible compared for the loads' currents.

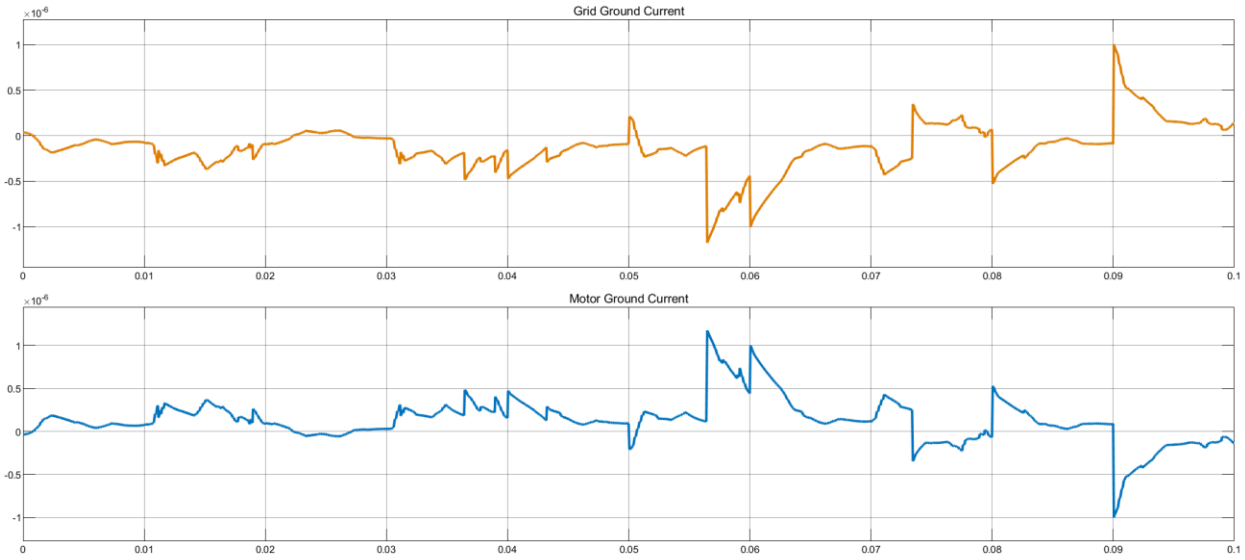

Figure 64 Leakage Currents When Grid Is Connected in THISPWM

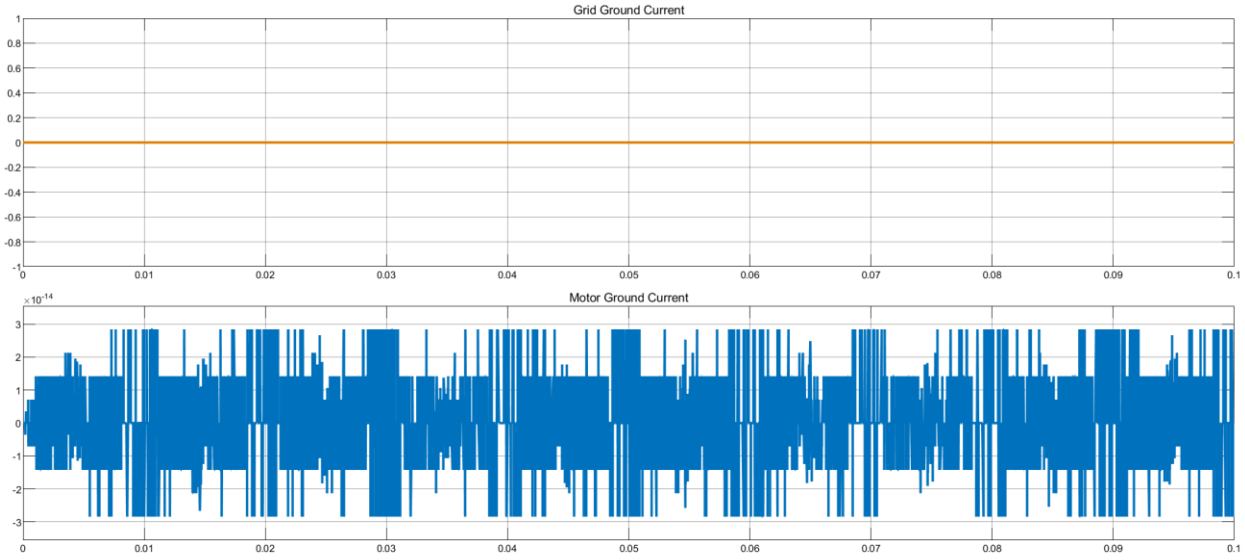

Figure 65 Leakage Currents When Grid Is Disconnected in THISPWM

4.1.2.7.2 Leakage Current in SVM Case

As the figures below show, a small leakage current to the order of 10^{-6} A is present when the grid is connected while dual inverter drive operation. However, these currents decease to zero and the overall circuit preserves neutrality all time. In the second case, when the grid is disconnected, a very small leakage current to the order of 10^{-14} A still exist at the load grounding. However, it's negligible compared for the loads' currents. Thus, SVM has advantage in comparison with other modulation techniques in comparison of leakage current circulation.

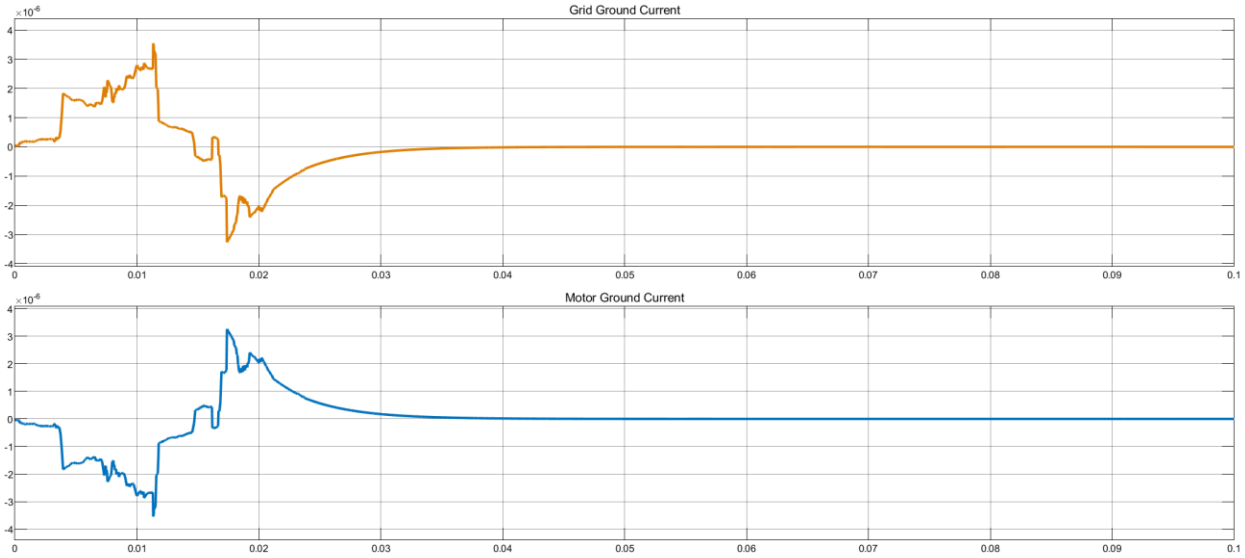

Figure 66 Leakage Currents When Grid Is Connected in SVM

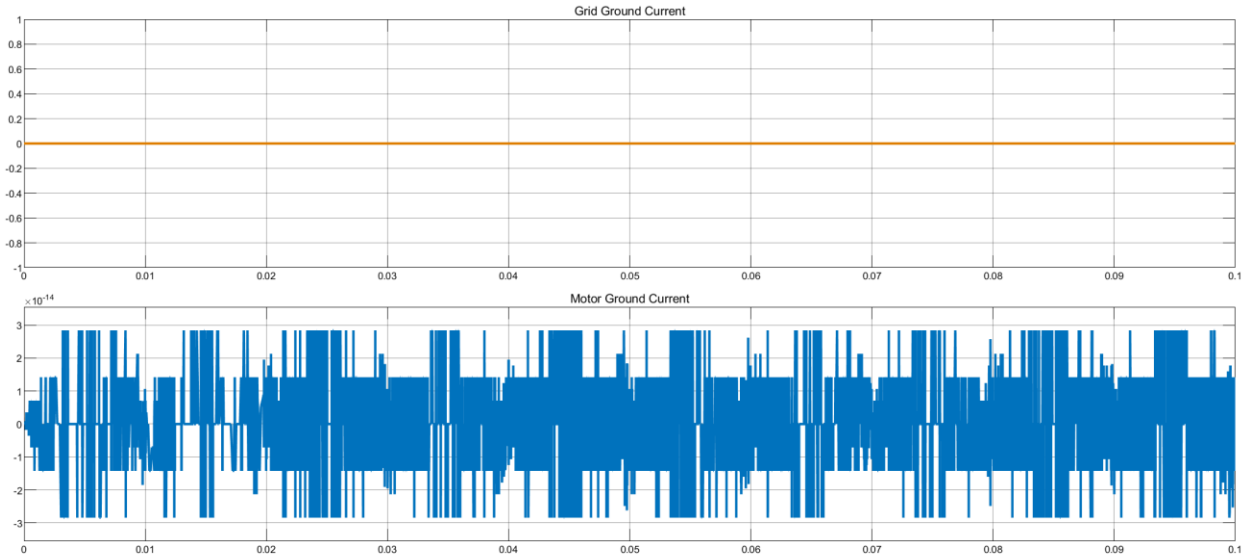

Figure 67 Leakage Currents When Grid Is Disconnected in SVM

4.1.2.7.3 Leakage Current Mitigation

One of the possible methods to eradicate the remaining leakage current when the grid is disconnected in SVM is by including a three-phase inductor in the circuit functioning as a filter. In this circuit, a 500 μH inductor was added.

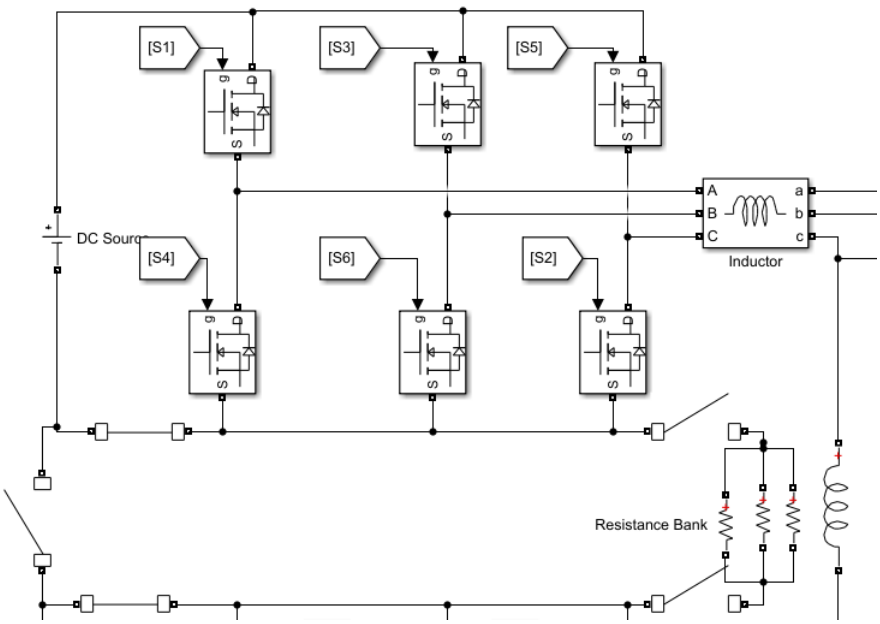

Figure 68 Adding Inductor to Dual Inverter Circuit

As a result, and under same circuit condition, the leakage current in the grounds came out to be zero.

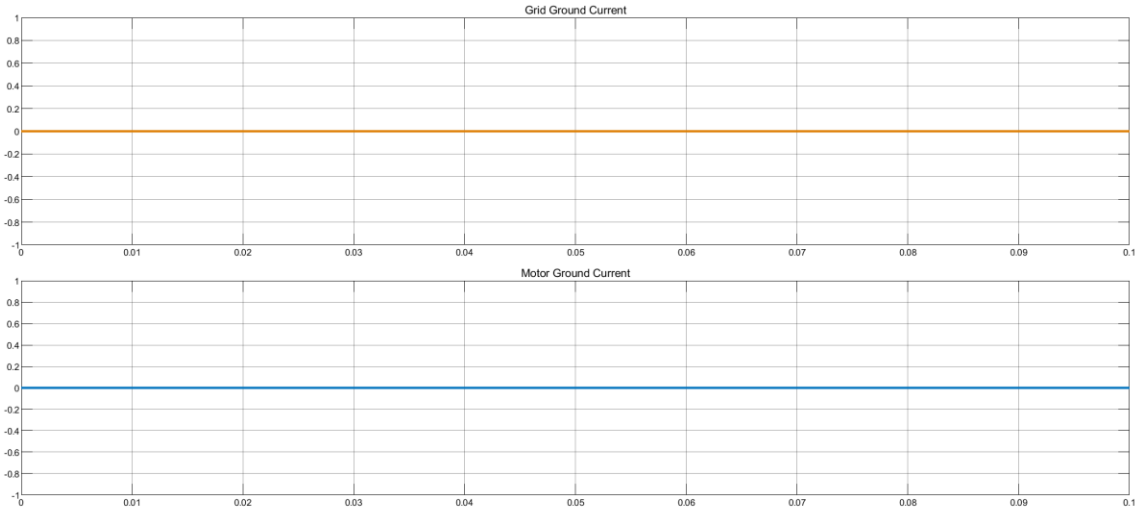

Figure 69 Leakage Currents When Grid Is Disconnected in SVM with Inductor Connection

4.1.2.8 Voltage Control

4.1.2.8.1 Method and Assumptions

In the previous examples, the gating of the inverters was independent of the output voltage value at the load. In order to achieve a better voltage contol, the output voltage should be linked to the gates of the inverters, causing the inverter to adapt and to provide the required switching output.

One of the possible ways is shown in the figure below. For simplicity, and to avoid the inductive effect of the load on the output voltage and current, few assumptions were made and implemented:

- Using the built-in Simulink universal bridges in the place of the three-phase inverters to minimze the size of the circuit.
- Using pure resistive loads (1Ω and 2Ω) to avoid the effect of inductance on voltage and current outputs.
- Using two DC voltage sources, each of 100 V.
- Adding a three-phase inductor of 500 μH to filter the output and obtain better sinosoidal waves.

The loop of the control circuit operates as follows:

- The value of the output voltage is normalized by dividing it by the gain K. K is carefully chosen to determine the desired output voltage.
- The voltage is transformed from the abc system to the dq0 system.
- The voltage is also measured to obtain the frequency and the angle.

- The d and q components are desired to be 1 and 0 respectively. In other orders, the voltage is required to flow just in the d axis direction.
- An integrator of value 100 is added to achieve the required output. The value of the integrator was chosen carefully to let the voltage reach the required value before the integrator saturation.
- Eventually, the dq0 signals are converted to abc system. Those are the input of a 6-pulse signal generator which is connected to the gates of the inverters.

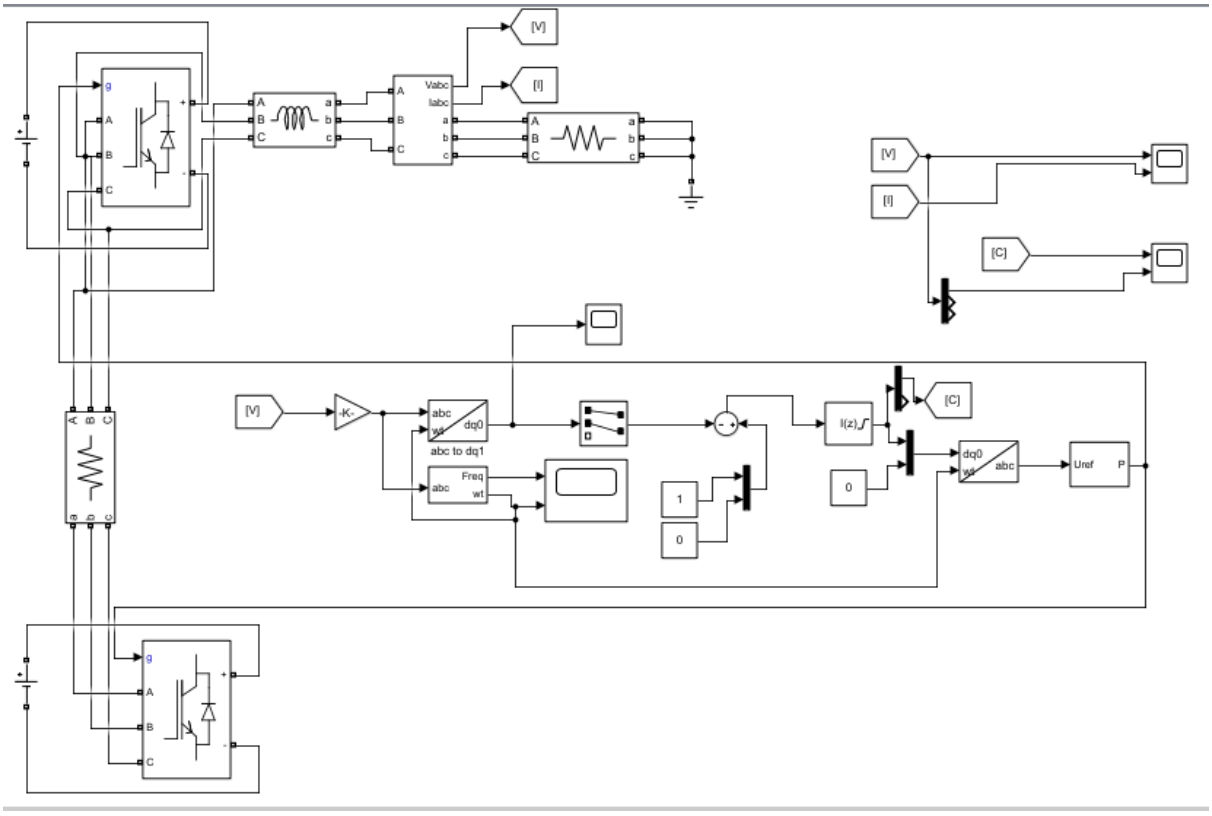

Figure 70 DQ0 Output Voltage Control of Dual Inverter Drive

4.1.2.8.2 Output Controlled Voltages in abc and dq0 Axes

Upon implementation of the control loop, the system reaches the desired motor output voltage value (50V).

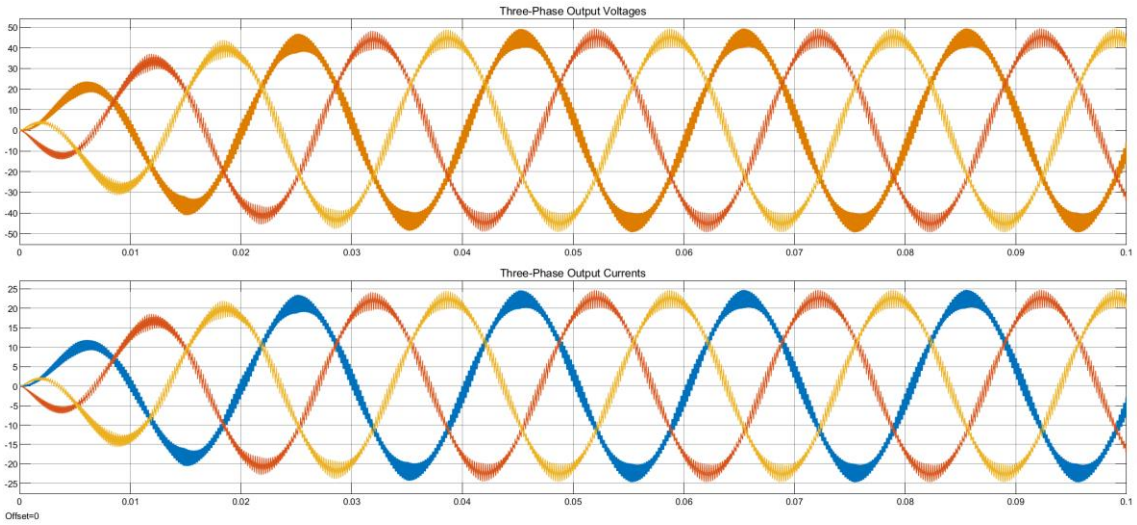

Figure 71 Controlled Output Voltages and Currents

The output voltage reaches 50V before the integrator saturation.

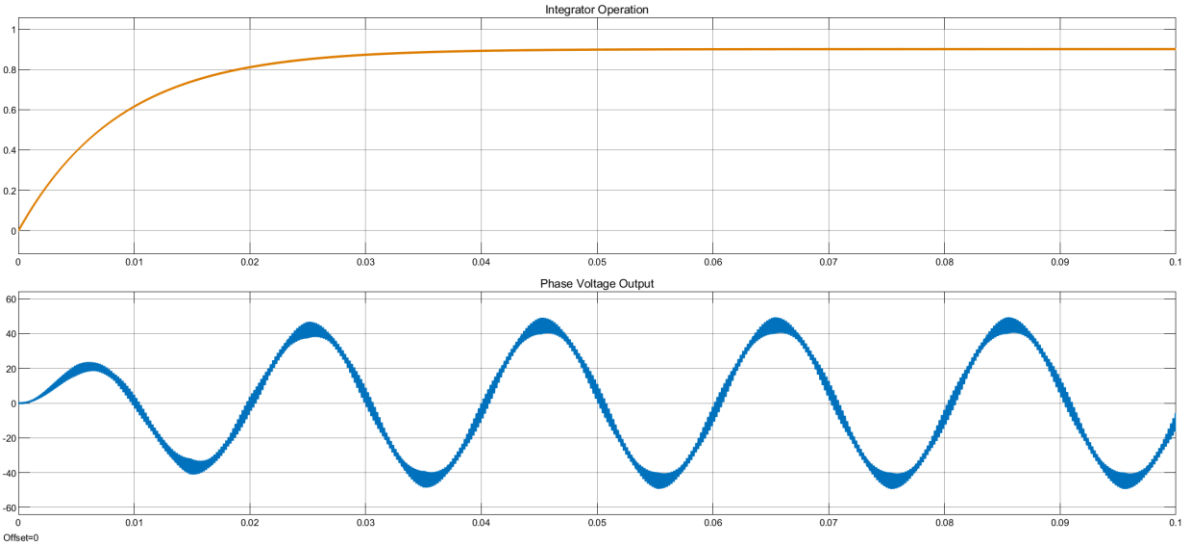

Figure 72 Integrator Operation in Comparison with Output Voltage

The D and Q axes voltages reach the desired values despite some ringing (noise due to nonlinearities).

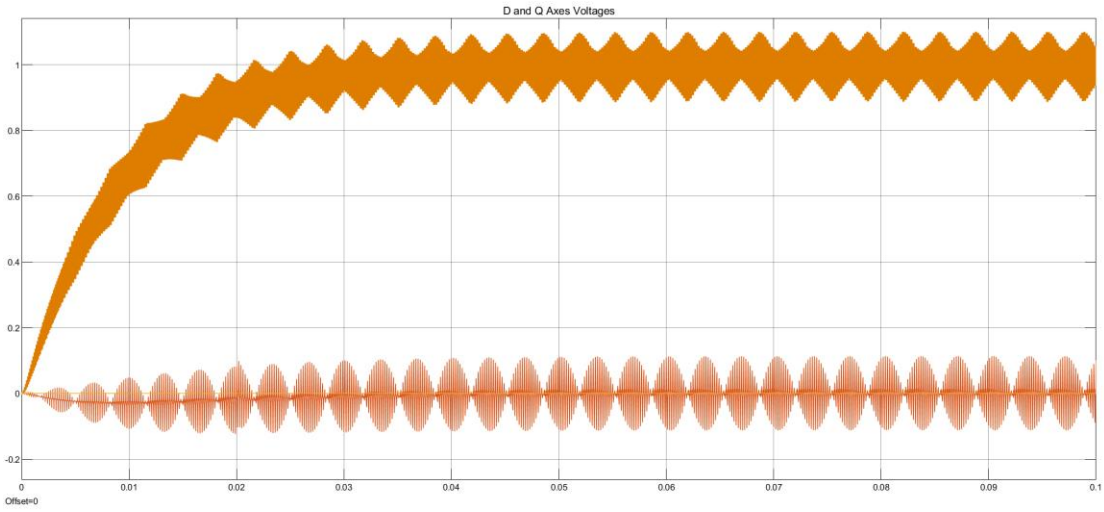

Figure 73 D and Q Axes Normalized Voltages

5.0 Conclusion

5.1 Remarks

- Modulation techniques of three phase inverter apply to the dual inverter drive. However, they operate in a similar way to the single inverter and do not achieve even or required output voltages and currents unless control techniques are involved. In comparison between SPWM, THISPWM and SVM, the latter two techniques are capable to give better results regarding voltage and harmonics. The THISPWM enables easy control through changing the modulation index and phase angle variation. However, the SVM gives the least switching losses, and it limits the leakage current flow in the circuit. The addition of a inductance as a filter can remove the remaining leakage current in case the grid was not connected and the currents are being dissipated through the load ground only.
- Phase angle variation can achieve desired voltage or power levels at different loads. When the phase angle between the gates of the two inverters was changed from 0 to 180 degrees, the voltage distribution and consequently the currents were changing significantly at the loads. At certain angle, equal phase voltage can be achieved at different loads. This principle applies also the active power distribution, reactive power distribution and total harmonic distortion. Another sort of voltage control can be applied by using feedback control and dq0 transformation over the output voltage.

5.2 Future Work

- Overmodulation and under modulation schemes: in all previous sections, the modulation index was considered to be 1. That means the carrier frequency and modulating signal have same amplitude. This may not be the case all time. If the modulation signal is lower than the carrier signal, it will be under modulated. If it is greater than the carrier signal, the modulated signal will be chopped. The figures below are examples of under modulated and overmodulated signals, of modulation signal 0.8 and 1.2 respectively.

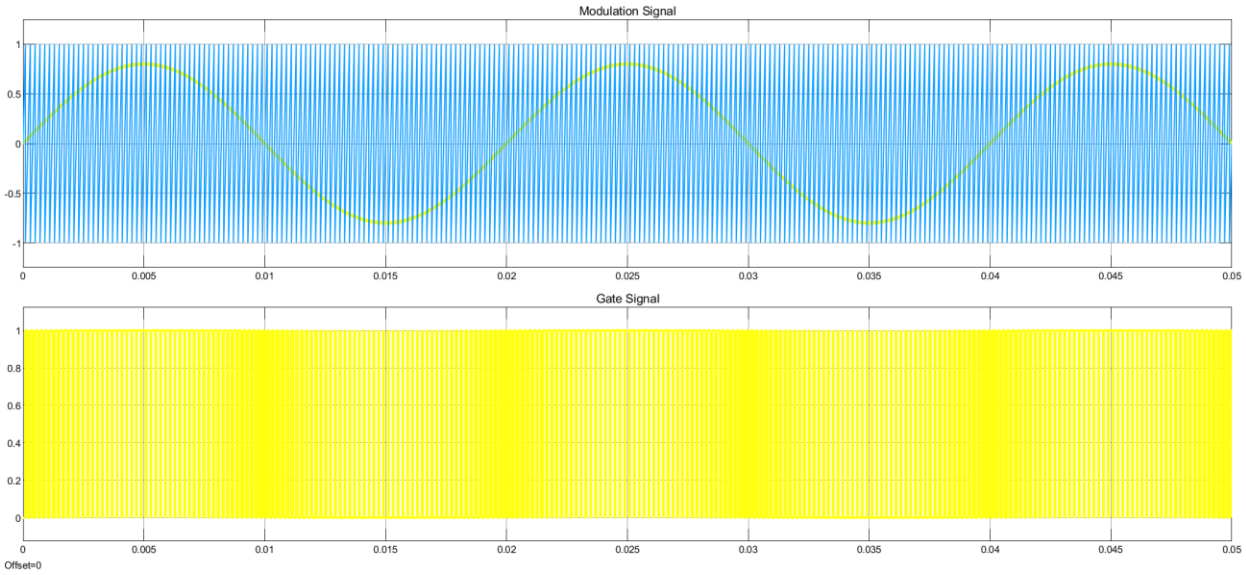

Figure 74 Undermodulated Signal of MI=0.8

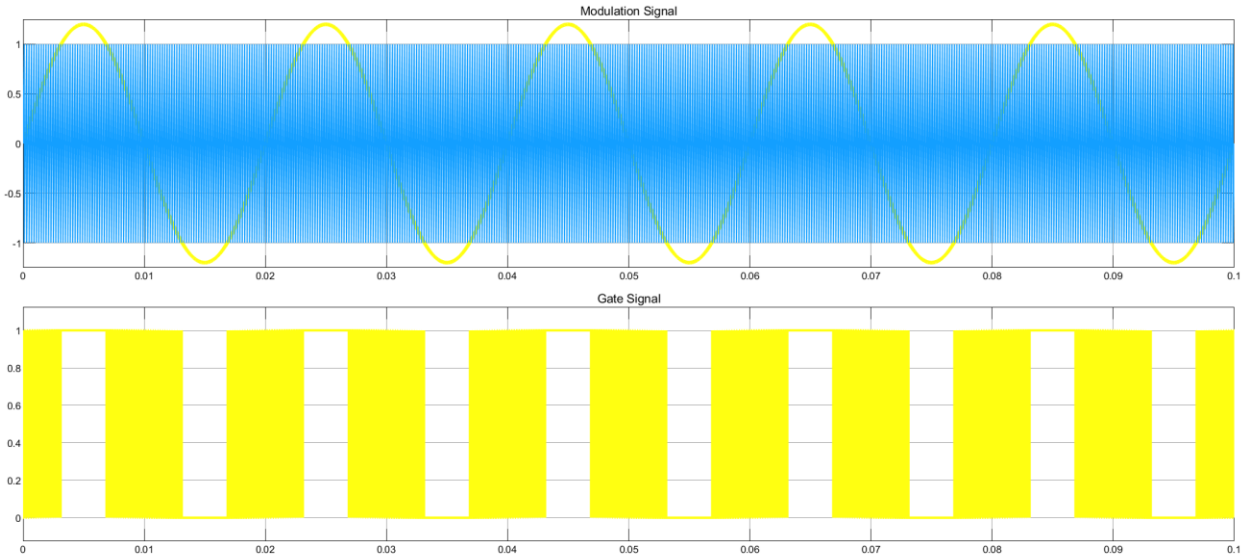

Figure 75 Overmodulated Signal of MI=1.2

- Discontinuous Modulation: in contrast to the regular PWM continuous techniques, the discontinuous mode involves switching 2 only of the 3 inverter poles. In some cases, it is called two phase modulation. By reducing the switching frequency, it aims to reduce the switching losses and harmonics. The voltage linearity depends on the location were the switch is kept inactive. The figure below shows the 60 degrees discontinuous PWM technique at 2 sectors.

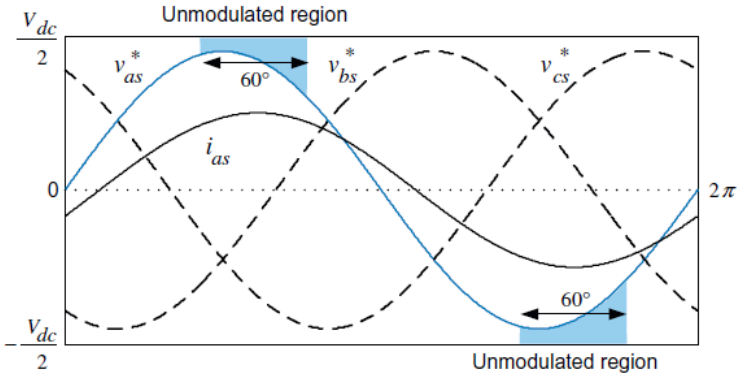

Figure 76 Unmodulated Sections of 60 Degrees DPWM [11]

- Hysteresis Control of Dual Inverter: hysteresis controllers aim to obtain effective control over the voltage or the current. They typically set a hysteresis band (h) which allows the switches to change their state to adapt for the current condition. If the variable reaches its upper limit, the regulator will switch off to decrease the value. If the variable reaches the lower limit, the regulator will turn on to increase the value of the variable.

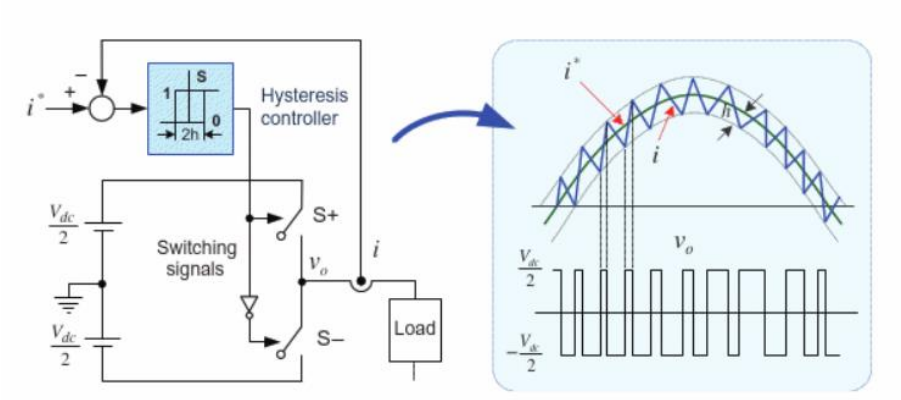

Figure 77 Principle of Hysteresis Regulator [11]

Bibliography

[1] H. C. Righolt and F. G. Rieck, "Energy chain and efficiency in urban traffic for ICE and EV," *2013 World Electr. Veh. Symp. Exhib. EVS 2014*, pp. 1–7, 2014, doi: 10.1109/EVS.2013.6914820.

[2] E. Bulut and M. C. Kisacikoglu, "Mitigating Range Anxiety via Vehicle-to-Vehicle Social Charging System," in *IEEE Vehicular Technology Conference*, 2017, doi: 10.1109/VTCSpring.2017.8108288.

[3] C. Viana, M. Keshani, and P. W. Lehn, "Interleaved buck-boost integrated dc fast charger with bidirectional fault blocking capability," in *2019 IEEE 20th Workshop on Control and Modeling for Power Electronics, COMPEL 2019*, 2019, doi: 10.1109/COMPEL.2019.8769656.

[4] M. Yilmaz and P. T. Krein, "Review of battery charger topologies, charging power levels, and infrastructure for plug-in electric and hybrid vehicles," *IEEE Transactions on Power Electronics*. 2013, doi: 10.1109/TPEL.2012.2212917.

[5] X. Zhou, G. Wang, S. Lukic, S. Bhattacharya, and A. Huang, "Multi-function bi-directional battery charger for plug-in hybrid electric vehicle application," *2009 IEEE Energy Convers. Congr. Expo. ECCE 2009*, pp. 3930–3936, 2009, doi: 10.1109/ECCE.2009.5316226.

[6] L. Zhou and M. Preindl, "Bidirectional Transformerless EV Charging System via Reconfiguration of 4×4 Drivetrain," *2018 IEEE Energy Convers. Congr. Expo. ECCE 2018*, pp. 3923–3927, 2018, doi: 10.1109/ECCE.2018.8558248.

[7] D. Thimmesch, "An SCR Inverter with an Integral Battery Charger for Electric Vehicles," *IEEE Trans. Ind. Appl.*, vol. IA-21, no. 4, pp. 1023–1029, 1985, doi: 10.1109/TIA.1985.349573.

[8] S. Haghbin, T. Thiringer, and O. Carlson, "An integrated split-phase dual-inverter permanent magnet motor drive and battery charger for grid-connected electric or hybrid vehicles," *Proc. - 2012 20th Int. Conf. Electr. Mach. ICEM 2012*, pp. 1941–1947, 2012, doi: 10.1109/ICElMach.2012.6350147.

[9] F. Lacressonniere and B. Cassoret, "Converter used as a battery charger and a motor speed controller in an industrial truck," in *2005 European Conference on Power Electronics and Applications*, 2005, doi: 10.1109/epe.2005.219286.

[10] R. Shi, S. Semsar, and P. W. Lehn, "Constant Current Fast Charging of Electric Vehicles via a DC Grid Using a Dual-Inverter Drive," *IEEE Trans. Ind. Electron.*, vol. 64, no. 9, pp. 6940–6949, 2017, doi: 10.1109/TIE.2017.2686362.

[11] S. H. Kim, *Electric Motor Control: DC, AC, and BLDC Motors*. 2017.

[12] P. H. Tran, “MATLAB/SIMULINK IMPLEMENTATION AND ANALYSIS OF THREE PULSE-WIDTH-MODULATION (PWM) TECHNIQUES,” 2012.

[13] J.-W. Jung, “PROJECT #2 SPACE VECTOR PWM INVERTER,” 2005.